Aalto University
School of Science

Master's programme in Mathematics and Operations Research

# Probabilistic Seismic Hazard Analysis for Nuclear Power Plant Sites in Finland

**Juhana Vehmas**

Master's Thesis
2024

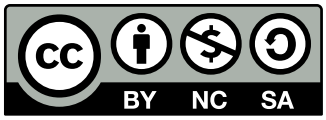

Aalto University
School of Science

**Author** Juhana Vehmas

**Title** Probabilistic Seismic Hazard Analysis for Nuclear Power Plant Sites in Finland

**Degree programme** Mathematics and Operations Research

**Major** Systems and Operations Research

**Supervisor** Prof. Ahti Salo

**Advisors** M.Sc. (Tech.) Jukka Koskenranta, M.Sc. (Tech.) Timo Leppänen

**Collaborative partner** Fortum Power and Heat Oy

**Date** 26 April 2024 **Number of pages** 53+9 **Language** English

**Abstract**

Probabilistic seismic hazard analysis (PSHA) is a method used to the estimate the likelihood of earthquake induced ground motions at a particular location. These estimates are then used to evaluate the risk to a structure such as a nuclear power plant (NPP). The latest PSHA for a Finnish NPP site located in Loviisa was made in 2021. Some significant sources of uncertainties and areas of development related to the modelling decisions made in the PSHA have been later identified.

This thesis seeks to study and develop the latest PSHA for the Loviisa NPP site. The PSHA model is also used to evaluate the seismic hazard in another Finnish NPP site located in Olkiluoto. The primary focus is on the Gutenberg-Richter (GR) parameters, which are used to describe the seisimic activity of a given region. A new declustered seismic catalog is adopted for the analysis, and the completeness of it is assessed in different parts of the study region. The GR parameters are estimated with a maximum likelihood method (MLE) method and with a least squares (LS) method, which was used in the PSHA from 2021.

Compared to the PSHA from 2021, a significantly larger amount of earthquake observations were utilized in this work. The GR parameters and the resulting hazard estimates show a high sensitivity to the completeness evaluation of the catalog and to the estimation method used for the GR parameters. The hazard estimates show a larger variation for the Loviisa site than for the Olkiluoto site. A suggestion is made to factor in these uncertainties into the analysis by extending the PSHA logic tree.

**Keywords** PSHA, Nuclear safety, Seismic hazard, Seismic catalog, Catalog completeness, Gutenberg-Richter, Loviisa, Olkiluoto

Aalto-yliopisto
Perustieteiden
korkeakoulu

**Tekijä** Juhana Vehmas

**Työn nimi** Todennäköisyysperusteinen seisminen hasardianalyysi Suomen ydinvoimaloiden laitospaikoille

**Koulutusohjelma** Mathematics and Operations Research

**Pääaine** Systems and Operations Research

**Työn valvoja** Prof. Ahti Salo

**Työn ohjaajat** DI Jukka Koskenranta, DI Timo Leppänen

**Yhteistyötaho** Fortum Power and Heat Oy

**Päivämäärä** 26.4.2024 **Sivumäärä** 53+9 **Kieli** englanti

**Tiivistelmä**

Todennäköisyysperusteinen seisminen hasardianalyysi (PSHA) on metodi, jota käytetään maanjäristyksen synnyttämien maan liikkeiden todennäköisyyksien arvioimiseen jollain tietyllä kohdealueella. Näitä todennäköisyysarvioita hyödynnetään rakennuksiin, kuten ydinvoimalaitokseen (NPP) kohdistuvan riskin arvioinnissa. Viimeisin seisminen hasardiarvio Loviisan ydinvoimalan laitospaikalle tehtiin vuonna 2021. Myöhemmin hasardiarviossa tehtyihin päätöksiin on tunnistettu liittyvän merkittäviä epävarmuuksia ja kehityskohteita.

Tämä diplomityö pyrkii tutkimaan ja kehittämään viimeisintä Loviisan laitospaikalle tehtyä seismistä hasardiarviota. Hasardiarviota varten kehitetyllä mallilla arvioidaan myös Olkiluodon ydinvoimalaitospaikan seismistä hasardia. Työssä keskitytään ensisijaisesti Gutenberg-Richter (GR) parametreihin, joilla kuvataan kohdealueen seismistä aktiivisuutta. Uusi seisminen deklusteroitu katalogi otetaan käyttöön, ja sen täydellisyyttä tarkastellaan eri puolilla tutkimusaluetta. GR parametrit määritetään suurimman uskottavuuden estimoinnilla (MLE) ja pienimmän neliösumman menetelmällä (LS), jota käytettiin vuoden 2021 hasardiarviossa.

Työssä hyödynnettiin huomattavasti enemmän maanjäristyshavaintoja kuin vuoden 2021 hasardiarviossa. GR parametrit ja niistä seuraavat hasarditulokset ovat hyvin herkkiä katalogin täydellisyystarkastelulle sekä GR parametrien estimoinnissa käytetylle metodille. Loviisan laitospaikan hasardituloksissa on enemmän vaihtelevuutta kuin Olkiluodon tuloksissa. Työssä ehdotetaan huomioimaan tunnistetut epävarmuudet laajentamalla laskennassa käytettyä logiikkapuuta.

**Avainsanat** Todennäköisyysperusteinen seisminen hasardianalyysi, ydinturvallisuus, seisminen hasardi, seisminen katalogi, Gutenberg-Richter, Loviisa, Olkiluoto

# Preface

This thesis was conducted at PRA team of Fortum Power and Heat Oy in collaboration with TVO. I would like to express my gratitude for Fortum and TVO for providing me this opportunity, and the PRA team for the great support and working atmosphere.

I am grateful for the continuous guidance and support from the thesis advisors Jukka Koskenranta and Timo Leppänen. I would also like to thank Timo Kukkola for the great feedback, and Päivi Mäntyniemi for the invaluable seismological expertise. Many thanks also to my supervisor Ahti Salo for the helpful meetings and feedback. Finally, I would like to thank my family and friends for supporting me throughout my studies at the university.

Espoo, 26 April 2024

Juhana Vehmas

# Contents

# Symbols and abbreviations

## Symbols

| | |
|---|---|
| $v(C > c)$ | Rate of exceedance |
| $c, C$ | Ground motion characteristic |
| $\lambda$ | Mean rate of occurence |
| $\sigma_\lambda$ | Standard deviation of the estimate of $\lambda$ |
| $T$ | Time interval length |
| $n(m)$ | Number of earthquakes with magnitudes greater than or equal to $m$ per unit of time |
| $a, \alpha$ | Intercept in the Gutenberg-Richter law, $\alpha = \ln(10)a$ |
| $b, \beta$ | Slope in the Gutenberg-Richter law, $\beta = \ln(10)b$ |
| $m_c$ | Minimum magnitude of completeness |
| $m_{\max}$ | Maximum magnitude |
| $m_{\min}$ | Minimum magnitude considered in the PSHA calculations |
| $n_c$ | Recurrence at $m_c$ |
| $n_{\min}$ | Recurrence at $m_{\min}$ |

## Abbreviations

| | |
|---|---|
| AFE | Annual Frequency of Exceedance |
| CENA | Central and Eastern North America |
| CI | Confidence Interval |
| CUVI | Cumulative Visual |
| DBE | Design Basis Earthquake |
| EPRI | Electric Power Research Institute |
| FMD | Frequency-Magnitude Distribution |
| GMPE | Ground Motion Prediction Equation |
| GR | Gutenberg-Richter |
| LS | Least Squares |
| MAXC | Maximum Curvature |
| ML | Maximum Likelihood |
| MLE | Maximum Likelihood Estimation |
| NPP | Nuclear Power Plant |
| PGA | Peak Ground Acceleration |
| PSHA | Propabilistic Seismic Hazard Analysis |
| SD | Standard Deviation |
| SA | Spectral Acceleration |
| SSC | Seismic Source Characterization |
| SSZ | Seismic Source Zone |
| STUK | Radiation and Nuclear Safety Authority |
| TVO | Teollisuuden Voima |
| UH | University of Helsinki |
| UHRS | Uniform Hazard Response Spectrum |

# 1 Introduction

In the pursuit of sustainable and secure energy future, nuclear power has a potential to be a stabilizing factor in the energy mix in which the share of variable renewables like solar and wind power is rising. In order to utilize this low-carbon potential of nuclear power, ensuring the safety is a vital concern throughout the entire lifespan of a nuclear power plant (NPP). In Finland nuclear safety is supervised by the Radiation and Nuclear Safety Authority (STUK). STUK specifies regulatory guides on nuclear safety and security, e.g. the guide YVL B7 [1] describes how internal and external hazards could be taken into account in the design of a NPP. External hazards include phenomena such as severe meteorological events, floods, fires, and seismic events like earthquakes.

In order to take earthquakes into account in the design of a NPP, the possible future on-site ground shaking caused by seismic events needs to be estimated. STUK requires the determination of a design basis earthquake (DBE) with anticipated frequency of occurrence being less than once in a hundred thousand years ($10^{-5}$/year). This DBE and the resulting on-site ground motions are used as the basis for the NPP safety design against earthquakes. The impact on the NPP site by the DBE is presented as a ground response spectrum. The ground response spectrum describes the maximum vibrations of damped single-degree-of-freedom oscillators assumed to be attached on ground at several natural frequencies [2].

The uncertainties related to size, location and resulting ground vibrations for future earthquakes can be taken into account by modelling the ground motion spectrum using a probabilistic approach. The uniform hazard response spectrum (UHRS) describes the ground motions at various frequencies, considering the probability of occurrence over a specified time period. Probabilistic seismic hazard analysis (PSHA) is a method that can be used to estimate the UHRS. In simple terms the idea of PSHA is to model and combine the results of how often earthquakes happen on nearby sources, and what kind of ground shaking is expected by those earthquakes. [3]

Finland has five operational nuclear units in two power plant sites as of 2024. Two units are located in the Loviisa plant owned by Fortum on the south coast of Finland, and three in the Olkiluoto plant owned by Teollisuuden Voima (TVO) on the west coast of Finland. Seismic studies concerning these plants have been made since the late 1980's and the safety of them against earthquakes is based on PSHA [2].

The latest PSHA for Loviisa site was made in 2021 [4]. STUK has made some remarks considering new modelling decisions and data used in the hazard analysis. The effect of some of these decisions for the hazard estimates for both Loviisa and Olkiluoto, has been later investigated further in a Master's thesis [5]. In [5] it was found that when estimating parameters for the earthquake occurrence with maximum likelihood estimation (MLE) instead of least squares (LS) regression, the seismic hazard predictions decrease significantly. This was also verified and studied in a special assignment [6]. The goal of this thesis is to further develop and update the latest PSHA from 2021, by focusing on the recommendations and findings made in

the previously mentioned studies. In addition, the modifications to the model are done by taking into account a new earthquake catalog [7] and completeness evaluation.

The basic principles and earlier research of PSHA are discussed in Chapter 2. Chapter 3 introduces the previous PSHA model, the new data and the methods used in this thesis. The results are presented and analysed in Chapter 4. Lastly, the findings and conclusions are discussed in Chapter 5.

# 2 Probabilistic Seismic Hazard Analysis

The foundations of PSHA were created by Cornell [8] in the 1960's. He acknowledged the importance of estimating the probabilities of possible future failures for infrastructure, caused by earthquake induced ground motion. Cornell proposed methods on how to derive the probabilistic seismic hazard from the relationships between earthquake occurance rates, locations and the induced ground motions at a site [9]. While there has been extensive debate about the use of PSHA, the imperative for quantitative measure of seismic hazard that can be used when analysing the safety of a structure, tends to overweight the challenges associated with the method [10]. Today, PSHA is still widely used and multiple implementations for different applications have been made [11, 12, 13].

PSHA intends to find the rates $\nu(C > c)$ with seismic characteristic $C$ exceeding varying levels of $c$ at the given site. Commonly used characteristic in PSHA are peak ground acceleration (PGA) and spectral acceleration (SA). PGA is defined as the maximum acceleration of the ground motion at a specific location during an earthquake, while SA considers that the maximum acceleration varies across different frequencies. SA is the maximum acceleration received in a damped single degree of freedom oscillator subjected to ground motion.

Calculating the rates of exceedance requires several steps. In simple terms, these steps outline the procedural workflow as follows [3]:

1. Identify earthquake sources with potential to produce ground motions at the site.
2. Describe each source by specifying the rates at which earthquakes of a particular magnitude are anticipated to occur in that source.
3. For each source define the distribution of distances from the source to the site of interest.
4. Establish the relationship between ground motions at the site and the earthquake's magnitude and distance.
5. Combine the results probabilistically by taking into account uncertainties related to each step.

Parts 1-3 can be seen as part of Seismic Source Characterization (SSC). SSC is a procedure of determining the location, size and likelihood of earthquakes relevant for the hazard analysis. In part 4 Ground Motion Prediction Equations (GMPE) are formed to predict the possible ground shaking at the site caused by the earthquake scenarios defined in SSC. The final step is to combine the SSC and the ground motion model, and integrate over all possible rupture scenarios.

## 2.1 Seismic Source Characterization

The first step of PSHA is to identify potential seismic sources and to characterize their seismic behaviour. The source can be a single fault, identified by its geological and

seismic properties. In less seismic regions in which faults are not as identifiable, the seismic source can be defined as a zone in which the seismic activity is assumed to be uniformly distributed, i.e. diffused seismicity [3]. Given the low seismic activity in Finland this thesis focuses on seismic source zones (SSZ).

### 2.1.1 Catalog Homogenization and Declustering

The seismic source characterization requires a comprehensive earthquake catalog that includes information of the seismic events in the study region. The earthquake catalog has to undergo several processing steps before it can be used as an input in the hazard calculations.

The size and energy release of an earthquake is commonly quantified using a magnitude scale. Although there are several magnitude scales, the earthquake information used for hazard assessments should be based on an uniform magnitude measure. This process of converting different scales of magnitudes in the catalog into a single magnitude scale is called magnitude homogenization. The selected magnitude scale should be consistent with the equations used for ground motion predictions. A widely used magnitude scale for seismic hazard applications is moment magnitude (Mw), which was introduced by Hanks and Kanamori in 1979 [14].

Seismic hazard analysis applications often rely on the assumption that seismicity can be described by a Poisson process [15]. This assumption implies that the seismic events in the catalog should not be spatially or temporally dependent on each other. The procedure of separating dependent events like fore- and aftershocks from the largest mainshock is known as declustering. Two widely used declustering methods were developed by Gardner and Knopoff in 1974 [16] and by Reasenberg in 1985 [17]. The method of Gardner and Knopoff utilizes time windows and distance limits to determine if an event is a aftershock for a larger mainshock or a dependent event.

### 2.1.2 Catalog Completeness

In addition to the homogenization and declustering, the completeness of the earthquake catalog must be evaluated to ensure that the catalog provides a representative and unbiased view of seismic activity in the study region. Complete reporting of earthquakes vary through time and space. The time period for which given magnitude earthquakes are assumed to be consistently recorded affects the activity rate estimates and the resulting PSHA.

A seismic catalog may contain instrumental and historical records. During an era of instrumental records, the completeness of data depends on the extent and density of the seismic monitoring network. The instrumental data is supplemented with historical observations made before the instrumental era. Because larger earthquakes are more likely to be noticed and recorded than the smaller ones, the period for complete reporting is usually longer for large magnitude earthquakes. However, as the historical records are derived from human observations, earthquakes occurring in unpopulated areas are less likely to be documented. [18]

The aim of completeness analysis is to determine the year after which a given magnitude is completely reported in a given zone. Two commonly employed approaches include a technique called Cumulative Visual (CUVI) method [19] as cited in [13], and a method proposed by Stepp in 1972 [20] that relies on the assumption of stationarity in earthquake occurrences. In both methods, the events are grouped into magnitude intervals (or bins), and the completeness analysis is conducted groupwise. In CUVI-method, the cumulative number of earthquakes for a given magnitude group are plotted against time, and the point in which the cumulative curve can be estimated by a straight line, indicates the starting point for the completeness period.

In the method proposed by Stepp [20], each magnitude group is modelled as a stationary Poisson point process in time. The mean rate of occurrence $\lambda$ of events in the magnitude group is estimated with different time interval lengths $T$, starting with the most recent interval. The estimate $\lambda$ is calculated as the total number of events in the interval divided by the corresponding interval length. The standard deviation of the estimate $\lambda$ is defined as

$$\sigma_\lambda = \frac{\sqrt{\lambda}}{\sqrt{T}}. \tag{1}$$

Since the assumption of stationarity, it is expected that $\lambda$ is approximately constant and $\sigma_\lambda$ should vary as $\frac{1}{\sqrt{T}}$ if the catalog is complete. Thus, the complete time period for each magnitude group can be determined by finding the interval in which $\sigma_\lambda$ behaves as $\frac{1}{\sqrt{T}}$.

The smallest magnitudes may be incompletely detected and recorded even at the present time. Thus, the magnitude above which it is assumed that all of the earthquakes in the given zone are reliably detected, should be determined. This is commonly referred as the threshold magnitude or as the minimum magnitude of completeness $m_c$.

Wyss et al. [21] and Wiemer and Wyss [22] proposed a straightforward approach for estimating $m_c$. The estimation is done by finding the point of maximum curvature (MAXC) in the cumulative frequency-magnitude distribution (FMD). FMD shows the counts of seismic events as a function of magnitude. The counts can be presented in incremental (non-cumulative) or cumulative form. In cumulative FMD the counts are summed cumulatively from the largest to the smallest observed earthquake. The point of MAXC in the cumulative FMD corresponds to the maximum value in the incremental FMD. As already noted by Wiemer and Wyss [22], MAXC gives a good first estimate for $m_c$, but tends to underestimate it on regions where the FMD curves with a slow rate.

### 2.1.3 Earthquake Recurrence

Today known as the Gutenberg-Richter (GR) law, Gutenberg and Richter [23] proposed that the number of earthquake occurrences and magnitude in any given region and

time period follows the relationship

$$\log_{10}(n(m)) = a - bm, \tag{2}$$

where $n(m)$ is the number of events with magnitude greater than or equal to $m$, and parameters $a$ and $b$ need to be assessed based on the earthquake observations in the specific source. Inserting $m = 0$ into Equation (2), gives us the the total number of earthquakes $10^a$. Thus parameter $a$ represents the total seismicity in the zone, while $b$ characterizes the rate of decrease in the frequency of earthquakes with increasing magnitude. Equation (2) can be expressed in exponential form

$$n(m) = e^{\alpha - \beta m}, \tag{3}$$

where $\alpha = \ln(10)a$ and $\beta = \ln(10)b$. As discussed earlier, the smallest earthquakes may be incompletely reported, thus only those observations with magnitudes larger or equal to $m_c$ should be taken into account in the parameter estimation. Also, Equations (2) and (3) imply that earthquakes with arbitrarily large magnitudes are possible, which contradicts experience [24]. To account for the lower and upper magnitude limits, the truncated GR law is expressed as

$$n(m) = n_c \frac{e^{-\beta(m-m_c)} - e^{-\beta(m_{\max}-m_c)}}{1 - e^{-\beta(m_{\max}-m_c)}}, \tag{4}$$

where $n_c = n(m_c)$. The upper limit for magnitude $m_{\max}$ represents the maximum magnitude a seismic source is capable of producing. There exist several techniques to assess the maximum magnitude. The maximum magnitude can be based on the geophysical properties of the source e.g. [25] or it can be estimated using statistical techniques e.g. [26].

The parameter estimation of GR law is an important part of PSHA because the estimated parameters define the rates at which earthquakes of a particular magnitude are anticipated to occur in a given source. Numerous techniques for the estimation of parameters have been proposed over the years, with perhaps the most used methods relying on maximum likelihood (ML) estimation. Aki [27] in 1965 was the first one to propose a ML estimate for $\beta$. This method assumes magnitude as a continuous variable, and does not include information about the differing level of completeness along the earthquake observations in the catalog.

In PSHA applications, the earthquake data is often binned by magnitude, and as discussed in the previous Section, the completeness may differ with magnitude. With differing level of completeness, the estimation becomes more complex. Weichert [28] formulated ML estimates and their uncertainties, taking into account unequal completeness periods for different magnitude bins. In Weichert's formulation the correlation between the estimates is absent. A maximum likelihood estimation (MLE) method that also estimates the correlation between the parameters $\alpha$ and $\beta$ (or $a$ and

$b$) was proposed by Stromeyer and Grünthal [29]. Moreover, the derived MLE method by Stromeyer and Grünthal is applicable for larger magnitude bins, as it does not rely on assumptions about the size of the magnitude bin.

Occasionally a linear least squares (LS) regression is used to estimate the GR parameters. LS was used already by Gutenberg and Richter [23]. Also Stepp [20] utilized LS estimation after assessing the completeness of an earthquake catalog. In the LS method the incompleteness is taken into account by dividing the number of observations in each magnitude bin by the corresponding completeness period. To evaluate the number of events with magnitude greater than or equal to $m$ in Equation (2), these completeness-corrected observations are summed cumulatively from the largest to the smallest observed magnitude bin. Finally, a line is fitted to the datapoints to estimate the parameters $a$ and $b$. The utilization of LS has been later criticized, as it does not take into account magnitude bins with zero observations at the high-magnitude end, therefore ignoring relevant information [28]. Another argument against LS is that when it is used for the cumulative datapoints, the general regression analysis assumption of independent observations is violated [30].

## 2.2 Ground Motion Prediction Equations

Ground motion prediction equations are used to estimate the ground motions at the site, given an earthquake occurrence. Rather than producing a single value estimate, GMPE provides a probability distribution for the characteristic $C$. Given an earthquake with magnitude $m$ and distance $r$ from the site, the probability of exceeding level $c$ at the site is expressed as

$$P(C > c \mid m, r). \tag{5}$$

The intensity of the ground shaking generally increases as a function of magnitude and decreases as a function of distance. In addition to magnitude and distance, GMPEs often include other explanatory variables such as the local site conditions and the fault mechanism type [31]. The relation between the ground shaking and the explanatory variables varies depending on the tectonic and geologic setting of the region. GMPEs have been developed since the 1960s to characterize ground motions in different parts of the world [32]. In more stable regions such as Finland, the scarcity of data complicates the development of appropriate GMPEs.

## 2.3 Hazard Calculations

Once the seismic activity of a seismic source is characterized and the appropriate ground motion model established, the seismic hazard induced by a source can be estimated. If a single source is considered, the exceedance rate at the site can be estimated as

$$v(C > c) = n_{\min} \int_{m_{\min}}^{m_{\max}} \int_{r_{\min}}^{r_{\max}} P(C > c \mid m, r) f_M(m) f_R(r)\, dr dm, \tag{6}$$

where $f_R(r)$ and $f_M(m)$ are probability density functions (PDFs) for distance and magnitude, $P(C > c \mid m, r)$ comes from the ground motion model and $n_{\min}$ is the recurrence rate of earthquakes greater than $m_{\min}$. The PDF for the truncated Gutenberg-Richter distribution is

$$f_M(m) = \frac{\beta e^{-\beta(m - m_{\min})}}{1 - e^{-\beta(m_{\max} - m_{\min})}}, \tag{7}$$

where $m_{\min}$ and $m_{\max}$ are the integration limits for magnitude in Equation (6). It should be noted that $m_{\min}$ is not the same minimum magnitude used in the estimation of GR parameters. In the hazard calculations, earthquakes with magnitudes smaller than $m_{\min}$ are ignored, because it assumed that they do not have the potential to produce ground shaking at levels that could cause damage [33].

For SSZs, for which the seismicity is assumed to be uniformly distributed, $n_{\min}$ is divided by the area of the SSZ, and the distance distribution $f_R(r)$ is directly determined by the geometry and location of the SSZ. However, the definition of $r$ is not entirely unambiguous. Some examples of distance measures are the distance to the earthquake epicenter and the distance to the hypocenter [34]. Hypocenter is the location within the Earth where the earthquake originates and epicenter is the location on the Earths surface directly above the hypocenter. The distance measure selected for the hazard integration should be consistent with the distance measure used for the GMPE.

To calculate the hazard from multiple sources, the exceedance rates from all of the sources are summed together. These total exceedance rates $v(C > c)$ are then calculated for multiple values of $c$ and with different frequencies. In practical applications, a numerical solution for the Equation (6) is found by the discretization of integrals.

The uncertainty related to PSHA calculations can be seen divided into two components: aleatory variability and epistemic uncertainty [35]. The aleatory component arises from the random nature of the seismic process and it is directly assessed via the probability distributions in Equation (6). The epistemic uncertainty originates from the lack of knowledge, and it is often incorporated into the analysis with a logic tree approach, first introduced by Kulkarni et al. [36]. In the logic tree approach, a set of possible values and weights are defined for the parameters in the hazard model. Then the hazard is calculated for each parameter value combination, and the product of weights presents the degree-of-belief for that particular combination. The mean hazard and the fractiles can be then estimated from the set of weights and hazard estimates obtained from the logic tree branches.

To change from rates and frequencies to probabilities, a Poisson distribution of events is assumed. If $v(C > c)$ is the annual frequency of exceedance (AFE) for a site, the probability of having at least one occurence with $C$ exceeding $c$ in $t$ years is

$$P(C > c \mid t) = 1 - e^{-v(C>c)t}. \tag{8}$$

# 3 Data and Methods

The focus in this thesis was on the development of a PSHA made in 2021 [4], referred in this thesis as PSHA2021. The PSHA2021 was conducted by Slate Geotechnical Consultants. In the PSHA2021 the hazard calculations were performed using a modified version of the computer program HAZ45 developed by Norman Abrahamson. The latest version of the original program is available on GitHub [37]. The modifications include new GMPEs and a magnitude reccurence relation with a varying $b$-value approach. This modified version was provided for Fortum by Slate, and it was adopted for this thesis.

## 3.1 Seismic Source Zones

In this thesis, the hazard analysis was performed with the same seismic source zone delineation used in the PSHA2021. These SSZs were outlined and described in an extensive seismological study made in 2016 by the Institute of Seismology at the University of Helsinki (UH) in cooperation with the Geological Survey of Finland, Geological Survey of Estonia, Geological Survey of Sweden and University of Uppsala [38]. Figure 1 shows the SSZ polygons and the Olkiluoto and Loviisa NPPs on a map. Source zones within a 300 km radius from the site of interest are taken into account in the hazard calculations.

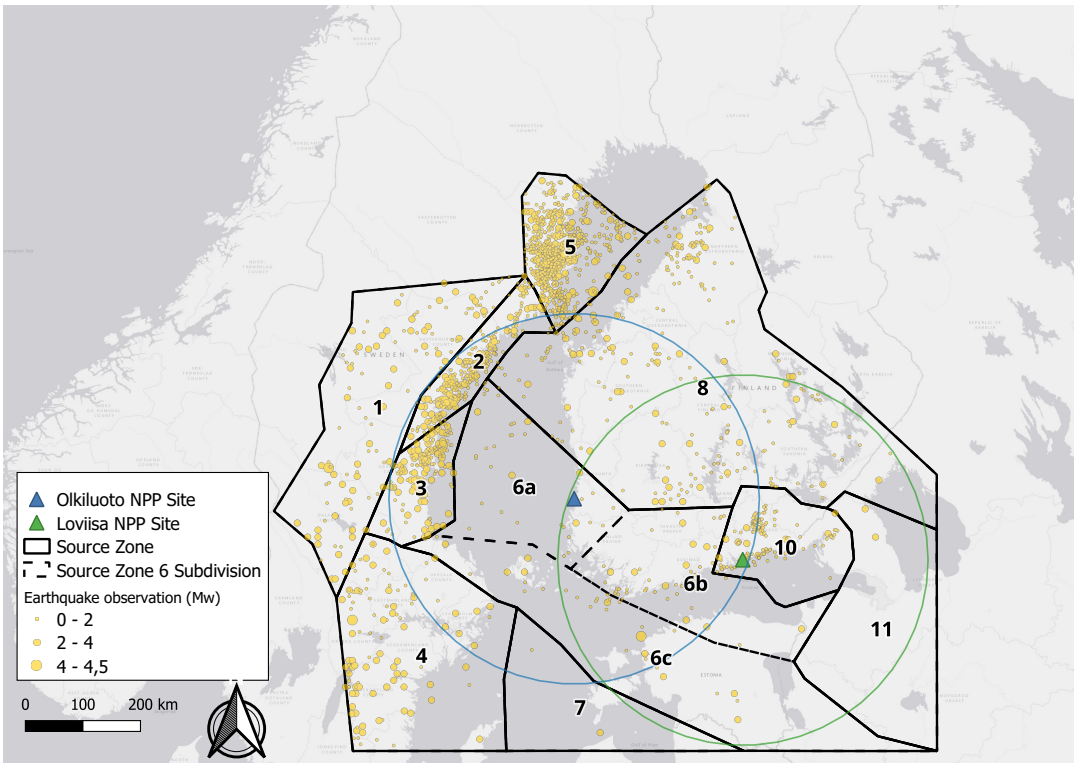


**Figure 1:** SSZs used in the PSHA2021 study [4] and the NPP sites. Circles with 300 km radius are drawn around the sites.

Based on the SSZ descriptions in the 2016 seismological study [38], the PSHA2021 defined a set of characterization parameters for each zone. These parameters, their input values and the corresponding logic tree weights are in Table 1. The focal depth for each SSZ was defined as a triangular probability distribution with a mode equal to approximately two-thirds of the maximum seismogenic thickness.

In addition to the characterization parameters in Table 1, the PSHA2021 used two separate distributions for the maximum magnitude $m_{\max}$. According to Slate, the first distribution is a modified version of a $m_{\max}$ distribution defined in a technical report [39] by Electric Power Research Institute (EPRI). The other distribution was used in a previous 2018 PSHA study [40] by Fortum, and was estimated by AFRY (former ÅF) [41, 42] applying the method of Kijko [26]. Both of these maximum magnitude distributions are in Table 2. The PSHA2021 characterization parameters and their weights in Tables 1 and 2 were utilized as-is in this thesis.

**Table 1:** Seismogenic thicknesses, fault plane dips, fault types and depth distributions for the SSZs. [4]

| SSZ | Seismogenic Thickness (km) [weight] | Fault Plane Dip (° from horizontal) [weight] | Fault Type | Focal Depth Triangular Distribution (km) [parameter] |
|---|---|---|---|---|
| 1 | 25 [0.2]<br>30 [0.6]<br>35 [0.2] | 80 [0.3]<br>85 [0.3]<br>90 [0.4] | Strike-slip | 0 [lower]<br>23 [mode]<br>35 [upper] |
| 2 | 22 [0.2]<br>26 [0.6]<br>30 [0.2] | 80 [0.3]<br>85 [0.3]<br>90 [0.4] | Strike-slip | 0 [lower]<br>18 [mode]<br>30 [upper] |
| 3 | 22 [0.2]<br>27 [0.6]<br>32 [0.2] | 80 [0.3]<br>85 [0.3]<br>90 [0.4] | Strike-slip | 0 [lower]<br>18 [mode]<br>32 [upper] |
| 4 | 21 [0.2]<br>26 [0.6]<br>31 [0.2] | 80 [0.3]<br>85 [0.3]<br>90 [0.4] | Strike-slip | 0 [lower]<br>18 [mode]<br>31 [upper] |
| 5 | 25 [0.2]<br>28 [0.6]<br>31 [0.2] | 80 [0.3]<br>85 [0.3]<br>90 [0.4] | Strike-slip | 0 [lower]<br>20 [mode]<br>31 [upper] |
| 6 | 18 [0.2]<br>23 [0.6]<br>28 [0.2] | 70 [0.2]<br>80 [0.2]<br>90 [0.6] | Reverse | 0 [lower]<br>15 [mode]<br>28 [upper] |
| 7 | 18 [0.2]<br>23 [0.6]<br>28 [0.2] | 80 [0.3]<br>85 [0.3]<br>90 [0.4] | Strike-slip | 0 [lower]<br>15 [mode]<br>28 [upper] |
| 8 | 19 [0.2]<br>25 [0.6]<br>30 [0.2] | 80 [0.3]<br>85 [0.3]<br>90 [0.4] | Strike-slip | 0 [lower]<br>17 [mode]<br>30 [upper] |
| 10 | 18 [0.2]<br>23 [0.6]<br>28 [0.2] | 80 [0.3]<br>85 [0.3]<br>90 [0.4] | Reverse | 0 [lower]<br>15 [mode]<br>28 [upper] |
| 11 | 18 [0.2]<br>23 [0.6]<br>28 [0.2] | 80 [0.3]<br>85 [0.3]<br>90 [0.4] | Strike-slip | 0 [lower]<br>15 [mode]<br>28 [upper] |

**Table 2:** Maximum magnitude distributions used in the PSHA2021 study [4]. Distributions are the same for each SSZ.

| EPRI-based [4] $m_{max}$ Distribution (Mw) [weight] | Fortum [40] $m_{max}$ Distribution (Mw) [weight] |
|---|---|
| 5.25 [0.01]<br>5.75 [0.08]<br>6.25 [0.23]<br>6.75 [0.36]<br>7.00 [0.32] | 5.5 [0.726]<br>6.0 [0.201]<br>6.5 [0.057]<br>7.0 [0.016] |

## 3.2 New Earthquake Catalog

The PSHA2021 used as a basis an earthquake catalog named UH (2016) from University of Helsinki covering events until the end of 2012, and supplemented it with events from 1.1.2013 until 30.12.2014. In this thesis an updated earthquake catalog [7] provided by UH was used. The catalog contains seismic observations starting from 1467 until the end of 2021. According to UH, it was compiled using the same main principles as was used for the UH (2016) catalog. The processing steps of the catalog are presented in detail in the 2016 seismological study by Korja et al. [38]. First a diverse set of magnitude scales in the initial data were homogenized and converted to moment magnitudes (Mw). After magnitude homogenization, a cluster analysis was performed to identify dependent events such as after- and foreshocks. According to UH, the declustering was performed following the methods of Gardner and Knopoff [16]. As the method is originally developed in a more active region with moderately large earthquakes, the windowing procedure utilized in the method was adjusted to better represent the low seismicity of the study region [38].

The catalog [7] provided by UH contained a total of 22 123 events. All of these events are classified as earthquakes, meaning that the catalog does not contain events of non-seismic origin such as explosions. From these earthquakes in the provided catalog, 591 events identified in the declustering process as after- or foreshock were filtered out. From the declustered catalog, 592 events without homogenized magnitude information and 103 events with homogenized magnitude smaller than zero were filtered out. Most of the events without homogenized magnitude located in Norway and thus outside the study region. After these steps the catalog contained a total of 20 837 events.

A considerable number of the remaining events lie outside the regions of interest. Geographic information system application QGIS [43] was used to classify on which source zone the seismic event belongs. In total 2 617 events were found to lie inside study region (Table 3). Only 2 recorded events were found in both SSZ 7 and SSZ 11, which is clearly an insufficient number to estimate seismic parameters. The lack of observations reflect the low seismicity within the source zones 7 and 11, but may be also partly explained by incomplete detection capability [38]. As in the PSHA2021,

parameters from the neighbouring zone SSZ 6 were assigned for SSZs 7 and 11. This is a conservative decision, but based on the results of this thesis, it has only a moderate impact on the hazard estimates.

**Table 3:** The number of events, the mean and the maximum observed magnitude by SSZ. The events are from the declustered catalog, before any completeness analysis.

| SSZ | Number of events | Mean Observed Magnitude (Mw) | Maximum Observed Magnitude (Mw) |
|---|---|---|---|
| 1 | 123 | 1.96 | 4.2 |
| 2 | 332 | 1.60 | 3.9 |
| 3 | 189 | 1.95 | 3.6 |
| 4 | 116 | 2.16 | 4.5 |
| 5 | 1111 | 1.25 | 4.1 |
| 6 (whole) | 125 | 1.56 | 4.4 |
| 6a | 37 | 1.44 | 2.9 |
| 6b | 52 | 1.36 | 3.6 |
| 6c | 36 | 1.97 | 4.4 |
| 7 | 2 | 1.85 | 2.6 |
| 8 | 293 | 1.27 | 4.0 |
| 10 | 324 | 0.84 | 2.9 |
| 11 | 2 | 2.15 | 2.2 |
| **Whole region** | **2617** | **1.39** | **4.5** |

### 3.2.1 Completeness Analysis

In the PSHA2021 the completeness of the declustered catalog was evaluated simultaneously for the whole study region, and the resulting completeness periods were used in the parameter estimation for the individual SSZs. In this thesis the aim was to carry out a more detailed analysis by evaluating the completeness periods in individual source zones or in source zone groups. Also, in the previous PSHA the parameters of GR law were determined using earthquakes of magnitude 1 Mw and above, suggesting that the minimum magnitude of completeness $m_c$ is equal to 1 Mw and identical for each SSZ. The correctness of this decision was investigated in this thesis.

The analysis was initiated with the investigation of $m_c$. The most recent ten years of data, starting from the beginning of 2012, was used to evaluate the current minimum magnitude of completeness in each SSZ. The MAXC method was used for the estimation of $m_c$, and manual corrections were applied for zones in which the cumulative FMD did not have a clearly distinguishable maximum curvature point.

After the estimation of $m_c$ with the most recent data, the completeness analysis for larger magnitudes than $m_c$ was continued using the whole dataset. The method proposed by Stepp [20] was utilised in order to determine the completeness period and its length $t_i$ for magnitude interval $[m_i - \frac{1}{2}\delta m, m_i + \frac{1}{2}\delta m]$, where $i \in [1, I]$ is the index of the magnitude interval and $I$ is the total number of intervals. The parameter $m_i$ is

the center value and $\delta m$ the width of the magnitude interval. A constant magnitude interval width of 0.5 Mw was used. With a smaller width, it was concluded that the amount of observations in each magnitude interval would not be sufficient for a reliable analysis. Because the amount of data decreases further back in the past, different time increments were used to form the time intervals used in the analysis. More specifically, 5 year time increments were used to form the time intervals for the most recent 30 years, 10 year increments for the most recent 50 to 100 years and 20 year increments for intervals longer than 100 years.

As seen from Table 3 there are significant differences in the number of earthquake observations between different source zones. Given that SSZ 5 has considerably more observations than the other SSZs, it is anticipated that SSZ 5 would dominate the completeness evaluation if conducted using the entire dataset. However, in some zones small amount of data and its sparsity, especially at larger magnitudes, makes SSZ-specific completeness evaluations unreliable or even impossible. To address this problem, the completeness of the smallest magnitude events was evaluated separately for each SSZ, and a grouping of SSZs was used for the completeness evaluation of larger magnitude events. For the largest magnitude intervals in the catalog, the whole study region was used to estimate the completeness. The reasoning behind this approach is that the detection capability of larger earthquakes should not be as dependent on the local factors, such as the population density or the extent of the seismic monitoring network of the SSZ. Additionally, to study the sensitivity related to the completeness evaluation process, a second evaluation was performed by only using data from individual SSZs.

The SSZ groups used for the completeness evaluation were [1 and 4], [2 and 3], [5] and [6, 8 and 10]. The groups were formed based on the geographic location and magnitude distribution of each SSZ. Because the seismic monitoring network and the detection capability has been evolved at different rates between Finland, Sweden and Estonia [38], the national boundaries were also taken into account when forming the groups. SSZs from 1 to 5 locate in Sweden while majority of the surface area of SSZs 6, 8 and 10 locate in Finland. Furthermore, the SSZs in Sweden were grouped such that the number of earthquakes does not significantly differ between the sources within the group. Therefore, SSZ 5 was not joined into any group.

## 3.3 Earthquake Recurrence

The completeness intervals and minimum completeness magnitudes $m_c$ defined the completeness analysis were used in the estimation of GR parameters for each SSZ. A bin width of 0.5 Mw was used in the parameter estimation, consistent with the bin width employed for the completeness evaluation. Two different estimation methods were used. First the parameters were estimated with a LS method. LS method was taken into account in this study, since according to [5] and [6] it seems that LS was used in the PSHA2021. After the LS estimation, the MLE method presented in [5] and [6] was utilized to estimate a new set of parameters. Both of these methods are presented in this Section.

### 3.3.1 Least Squares

In order to estimate the $a$ and $b$ parameters, a least squares method was used to fit a linear regression model to the data. The equations for the LS method can be found, for example, in [44]. The LS estimates for Equation (2) are given by

$$b = -\frac{\sum_{i=1}^{I}(m_i - \overline{m})\left(\log_{10}(n(m_i)) - \overline{\log_{10}(n(m_i))}\right)}{\sum_{i=1}^{I}(m_i - \overline{m})^2}, \tag{9}$$

$$a = \overline{\log_{10}(n(m_i))} + b\overline{m}, \tag{10}$$

where $m_i$ is the center value of the magnitude bin $i \in [1, I]$, and the overline denotes mean value. Because the magnitude bins have different observation periods, the number of events in the bin should be divided with the corresponding completeness period length $t_i$. The $n(m_i)$ values of Equation (2) are then obtained by summing these annual rates cumulatively. Based on an example calculation [45] provided by Slate, all of the magnitude bins with zero observations were left out from the regression.

The variances and covariance of the LS estimates are defined as

$$\mathrm{var}(a) = \frac{\sigma^2 \sum_{i=1}^{I} m_i^2}{I \sum_{i=1}^{I}(m_i - \bar{m})^2}, \tag{11}$$

$$\mathrm{var}(b) = \frac{\sigma^2}{\sum_{i=1}^{I}(m_i - \bar{m})^2}, \tag{12}$$

$$\mathrm{cov}(a, b) = \frac{\sigma^2 \bar{m}}{\sum_{i=1}^{I}(m_i - \bar{m})^2}, \tag{13}$$

where the variance $\sigma^2$ is given by [45]

$$\sigma^2 = \frac{\sum_{i=1}^{I}\left(\log_{10}(n(m_i)) - \overline{\log_{10}(n(m_i))}\right)^2}{I^2}. \tag{14}$$

This $\sigma^2$, also used in the PSHA2021, differs from the ordinary least squares variance estimate, in which the variance is calculated as the sum of squared residuals divided by the degrees of freedom $I - 2$.

HAZ45 takes as an input the $b$-value and the value of the recurrence rate at minimum magnitude $m_{\mathrm{min}}$

$$n_{\mathrm{min}} = 10^{a - b m_{\mathrm{min}}}. \tag{15}$$

In addition to the mean estimate the confidence interval (CI) bounds for $n_{\min}$, and the corresponding $b$-values were inserted to HAZ45. Following the PSHA2021 example calculation [45], these bounds were calculated from

$$\left(n_{\min,L} = 10^{a_{\mathrm{L}} - b_{\mathrm{L}} m_{\min}},\ n_{\min,U} = 10^{a_{\mathrm{U}} - b_{\mathrm{U}} m_{\min}}\right), \tag{16}$$

where the lower and upper bounds for $a$ and $b$ are defined as

$$\left(a_{\mathrm{L}} = a - 1.65\sqrt{\mathrm{var}(a)},\ a_{\mathrm{U}} = a + 1.65\sqrt{\mathrm{var}(a)}\right), \tag{17}$$

$$\left(b_{\mathrm{L}} = b - 1.65\frac{\mathrm{cov}(a,b)}{\sqrt{\mathrm{var}(a)}},\ b_{\mathrm{U}} = b + 1.65\frac{\mathrm{cov}(a,b)}{\sqrt{\mathrm{var}(a)}}\right). \tag{18}$$

A weight of 0.6 was assigned for the mean estimate and a weight of 0.2 for both the lower and upper bound estimates.

### 3.3.2 Maximum Likelihood Estimation

The sensitivity of the PSHA2021 model was studied by Visakorpi [5] with a conclusion that the estimation of GR parameters using a MLE method instead of LS regression has a significant effect on the hazard estimates. In [5] derivation of a MLE method for the GR parameter estimation was shown. The method was verified and the equations rederived by Heikkilä [6]. Both of these derivations closely resemble the derivations made by Stromeyer and Grünthal [29], which in turn are close to those proposed by Weichert [28], but with different estimates for the variances $\mathrm{var}(a)$, $\mathrm{var}(b)$ and for the covariance $\mathrm{cov}(a,b)$.

Both Visakorpi [5] and Heikkilä [6] presented a MLE derivation for the truncated GR relation in Equation (4), but concluded that the truncation does not have an effect on the estimated parameters when the difference between $m_{\max}$ and $m_c$ is multiple units of magnitude. As this was always the case in the present thesis, a MLE for the non-truncated GR-relation in which the term $e^{-\beta(m_{\max}-m_c)}$ is approximated as zero was used. Also, in the present thesis a constant bin width $\delta m$ was used for each magnitude bin. For the sake of completeness, the equations from [6] with these modifications are presented below.

It is assumed that earthquakes follow a Poisson process. The probability $P(n_i)$ of observing $n_i$ events from magnitude range $[m_i - \frac{1}{2}\delta m, m_i + \frac{1}{2}\delta m]$ in time period $t_i$ can be then used to form the likelihood function

$$\mathcal{L} = \prod_{i=1}^{I} P(n_i) = \prod_{i=1}^{I} \frac{(\delta n_i t_i)^{n_i}}{n_i!} e^{-\delta n_i t_i}, \tag{19}$$

where $\delta n_i$ is the average rate at which events with magnitudes between $[m_i - \frac{1}{2}\delta m, m_i + \frac{1}{2}\delta m]$ occur. Using the non-truncated GR relation in Equation (3), the rate parameter can be expressed as

$$\delta n_i = n(m_i - \frac{1}{2}\delta m) + n(m_i + \frac{1}{2}\delta m) \tag{20}$$

$$= 2\sinh\left(\beta\frac{\delta m}{2}\right) e^{\alpha-\beta m_i}. \tag{21}$$

The GR parameter estimates, which maximize the log-likelihood function $\ln \mathcal{L}$, can be found by forming the partial derivatives with respect to $\alpha$ and $\beta$ and finding the roots for these derivatives. The solution for $\beta$ is given by

$$\sum_{i=1}^{I} n_i m_i = \frac{N \sum_{i=1}^{I} e^{-\beta m_i} t_i m_i}{\sum_{i=1}^{I} e^{-\beta m_i} t_i}, \tag{22}$$

where $t_i$ is the completeness period length for magnitude bin $i$, determined in the completeness analysis. Note that here $n_i$ is the observed value of earthquakes in the corresponding bin, and not the cumulative value used in the least squares method. $N = \sum_{i=1}^{I} n_i$ is the total number of earthquakes in range $[m_c, m_{\max}]$. The Equation (22) is the same as presented by Weichert [28], and it can be solved numerically. In this thesis, bisection method was used. After $\beta$ is found, $\alpha$ can be solved from

$$e^{\alpha} = \frac{N}{2\sinh\left(\beta\frac{\delta m}{2}\right)\sum_{i=1}^{I} e^{-\beta m i} t_i}. \tag{23}$$

The uncertainty of the estimated parameters is described with a covariance matrix $\boldsymbol{C}$. The covariance matrix is estimated as the inverse Hessian $\boldsymbol{H}$ of the negative log-likelihood function

$$\boldsymbol{C} = \begin{pmatrix} \mathrm{var}(\alpha) & \mathrm{cov}(\alpha,\beta) \\ \mathrm{cov}(\alpha,\beta) & \mathrm{var}(\beta) \end{pmatrix} = (-\boldsymbol{H})^{-1} = -\frac{1}{D}\begin{pmatrix} \frac{\partial^2 \ln \mathcal{L}}{\partial \beta^2} & -\frac{\partial^2 \ln \mathcal{L}}{\partial \alpha \partial \beta} \\ -\frac{\partial^2 \ln \mathcal{L}}{\partial \alpha \partial \beta} & \frac{\partial^2 \ln \mathcal{L}}{\partial \alpha^2} \end{pmatrix}, \tag{24}$$

where $D$ is the determinant of the Hessian

$$D = \left(\frac{\partial^2 \ln \mathcal{L}}{\partial \alpha^2}\right)\left(\frac{\partial^2 \ln \mathcal{L}}{\partial \beta^2}\right) - \left(\frac{\partial^2 \ln \mathcal{L}}{\partial \alpha \partial \beta}\right)^2. \tag{25}$$

The second order partial derivatives are

$$\frac{\partial^2 \ln \mathcal{L}}{\partial \alpha^2} = -N, \tag{26}$$

$$\frac{\partial^2 \ln \mathcal{L}}{\partial \beta^2} = \sum_{i=1}^{I} \left[ (n_i - \delta n_i t_i) \left( \frac{\delta m}{2} \right)^2 \left( 1 - \coth^2 \left( \beta \frac{\delta m}{2} \right) \right) - \delta n_i t_i \phi_i^2 \right], \tag{27}$$

$$\frac{\partial^2 \ln \mathcal{L}}{\partial \alpha \partial \beta} = - \sum_{i=1}^{I} \delta n_i t_i \phi_i, \tag{28}$$

where the term $\phi_i$ is defined as

$$\phi_i = \frac{\delta m}{2} \coth \left( \beta \frac{\delta m}{2} \right) - m_i. \tag{29}$$

Now the elements of the covariance matrix can be used to calculate the variances and covariance of $a$ and $b$

$$\mathrm{var}(a) = \frac{1}{\ln(10)^2} \cdot \mathrm{var}(\alpha) = \frac{1}{\ln(10)^2} \cdot \left( -\frac{1}{D} \frac{\partial^2 \ln \mathcal{L}}{\partial \beta^2} \right), \tag{30}$$

$$\mathrm{var}(b) = \frac{1}{\ln(10)^2} \cdot \mathrm{var}(\beta) = \frac{1}{\ln(10)^2} \cdot \left( -\frac{1}{D} \frac{\partial^2 \ln \mathcal{L}}{\partial \alpha^2} \right), \tag{31}$$

$$\mathrm{cov}(a, b) = \frac{1}{\ln(10)^2} \cdot \mathrm{cov}(\alpha, \beta) = \frac{1}{\ln(10)^2} \cdot \left( \frac{1}{D} \frac{\partial^2 \ln \mathcal{L}}{\partial \alpha \partial \beta} \right). \tag{32}$$

As proposed by Stromeyer and Grünthal [29], the uncertainties of $a$ and $b$ can be directly propagated to the recurrence rate $n(m)$ at any given magnitude. Additionally, following a technique by Miller and Rice [46], they suggested how to sample the probability distribution of the recurrence rate and set the logic tree weights in an statistically optimal manner. In this thesis three sampling points were used. Thus, a weight of 0.666 was assigned for the mean estimates and a weight of 0.167 for both the lower and upper bound estimates. The lower and upper bounds for $n_{\min}$ were calculated from

$$\left( n_{\min,L} = 10^{a - b m_{\min} - 1.73\sigma(m_{\min})},\ n_{\min,U} = 10^{a - b m_{\min} + 1.73\sigma(m_{min})} \right), \tag{33}$$

where $\sigma(m_{\min})$ is the standard deviation of $a - bm$ at the minimum magnitude, and is defined as

$$\sigma(m) = \sqrt{\mathrm{var}(a - bm)} = \sqrt{\mathrm{var}(a) + m^2 \mathrm{var}(b) - 2m\mathrm{cov}(a, b)}. \tag{34}$$

HAZ45 uses the $b$-value to extrapolate from the recurrence at minimum magnitude to the larger magnitudes. The lower and upper bounds for $b$ were defined as

$$\left(b_{\mathrm{L}} = b - 1.73\sqrt{\mathrm{var}(b)},\ b_{\mathrm{U}} = b + 1.73\sqrt{\mathrm{var}(b)}\right). \tag{35}$$

Unlike the LS method, the MLE method takes into account magnitude bins with zero observations. Thus a upper limit magnitude, up to which point the empty bins are considered, should be determined. The maximum magnitude distributions in Table 2 were utilized to define this upper limit. If a weight of 0.5 is given to both of the distributions, the weighted mean for the maximum magnitude is equal to 6.15 Mw. Thus, the magnitude bin 6-6.5 Mw was the last empty magnitude bin used in the MLE estimation.

## 3.4 Setup for Hazard Calculations

SSZs within 300km radius from the corresponding site were taken into account in the hazard estimation. For Loviisa site these zones are SSZs 6, 7, 8, 10 and 11, and the SSZs for Olkiluoto are 1, 2, 3, 4, 5, 6, 7, 8 and 10. Using the modified HAZ45 program, spectral acceleration was utilized as the intensity measure with 18 acceleration levels between 0.00001 and 5 g, where g is the gravitational acceleration. As SA is frequency dependent, the exceedance rates were calculates for 21 frequencies between 0.1 and 100 Hz.

In the PSHA2021, the minimum magnitude $m_{\mathrm{min}}$ for the hazard calculations was set to 4.5 Mw, and the corresponding recurrence rate $n_{\mathrm{min}}$ for each SSZ was picked from Equation (15) with the estimated parameters $a$ and $b$. The minimum magnitude was selected based on recommendations made by EPRI [47] and on expert judgment regarding the seismic capacity of Finnish NPPs [48]. Also, a method with a varying $b$-value was applied to the recurrences rates in the PSHA2021. In the hazard calculations the estimated $b$-value was used until Mw of 5.75, after which the $b$-value was set to 2. The minimum magnitude of 4.5 Mw and the split in the recurrence curve was also assumed in this thesis.

Figure 2 shows the logic tree structure used in the PSHA2021 study. A web-based diagram software draw.io [49] was used to illustrate the logic tree. As stated before, in the PSHA2021 the completeness periods were determined for the whole study region all at once, and LS was used for the recurrence estimation. In this thesis two set of completeness periods were determined. One in which the completeness of larger magnitudes was evaluated in a SSZ groups, and one without any SSZ grouping. Also, two methods were considered in the estimation of recurrence parameters. To study the effect of these modelling decisions to the recurrence parameters and to the resulting hazard, the calculations were first performed for each of the combination separately using the logic tree of PSHA2021. When using MLE method, the weights of the recurrence parameter estimates (Figure 2) were changed accordingly.

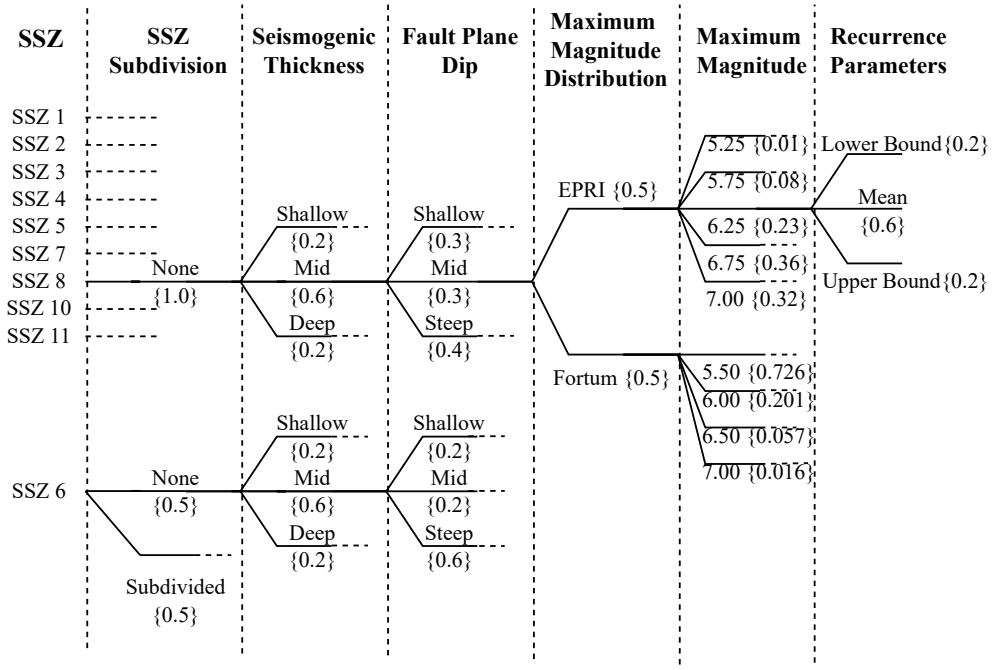


**Figure 2:** Logic tree used in the PSHA2021 [4] study, and in the present thesis to study the sensitivity to different earthquake completeness and recurrence estimation methods. The weights for the branches are given in braces.

Finally, the logic tree was extended to take into account the different uncertainties related to the recurrence parameter estimation. The extended logic tree is presented in Figure 3. A weight of 0.5 was assigned for both the LS and MLE method. Although the conventional LS method has been criticized, the recurrence estimation method used in the PSHA2021 was not completely ruled out, since at the time of writing this thesis the reasoning behind the method was not clarified by the authors of the PSHA2021. In addition to the main completeness analysis, conducted with the SSZ grouping, the completeness analysis without the SSZ grouping was taken into account with a weight of 0.25. A smaller weight was assigned for the latter analysis due to the sparsity of data in individual SSZs.

The ground motion model used in the PSHA2021 was utilized without modifications in this thesis. The model is based on the NGA-East GMPEs developed for the Central and Eastern North America (CENA) [50]. The NGA-East model was developed for frequencies ranging from 0.1 Hz to 100 Hz and it is suitable for hard rock conditions. It is applicable for moment magnitudes between 4 and 8.2, and covers distances of up to 1500 kilometers. The model consist of 17 GMPEs with a set of weights to be utilized in the logic tree approach. Slate [4] made an adjustment to the original GMPEs by changing the site condition parameter $\kappa$ that describes the attenuation of high frequency ground motions. The original NGA-East $\kappa$-value of 0.006 s was changed to a value of 0.015 s as the higher value was seen more appropriate for the study region [51].

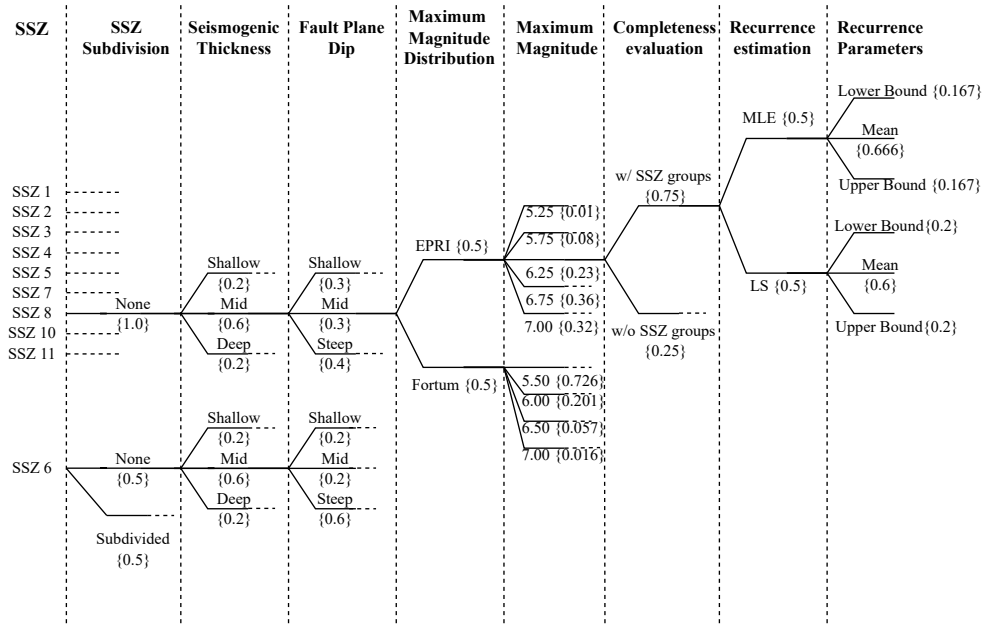


**Figure 3:** The final logic tree used for the hazard calculations. The weights for the branches are given in braces.

HAZ45 directly outputs the mean hazard estimate at each acceleration level. The mean is obtained by summing the hazard weighted by the corresponding logic tree branch weight. The median hazard and other fractile estimates were estimated from the HAZ45 output using Microsoft Excel. The following procedure was used form the hazard fractiles. First, for each branch in the logic tree, the hazard from individual SSZs were summed to present the total hazard from that particular branch. This means that instead of considering every single branch combination between the different SSZs, it is assumed that the parameters in each SSZ vary together. These total hazard values were sorted from smallest to largest with their corresponding branch weights. Based on the cumulative sum of these weights, the fractiles were picked from the sorted hazard values. Also, it should be noted that the output from the modified HAZ45 program does not contain hazard results for the individual branches in the GMPE logic tree. Instead it outputs the results by using the mean of the GMPE logic tree. Thus, the variation related to the GMPEs could not be properly utilized in the fractile estimation.

# 4 Results

## 4.1 Completeness Analysis

The ten most recent years of data in the catalog was used for studying the minimum magnitude of completeness. Figure 4 shows the frequency-magnitude distributions and the MAXC point for the SSZs with a bin width of 0.1 Mw. As we can see for most of the SSZs, there is a relatively distinct point where the cumulative FMD starts to curve. However, especially in SSZ 8 the FMD curves more gradually, making the MAXC estimation less reliable.

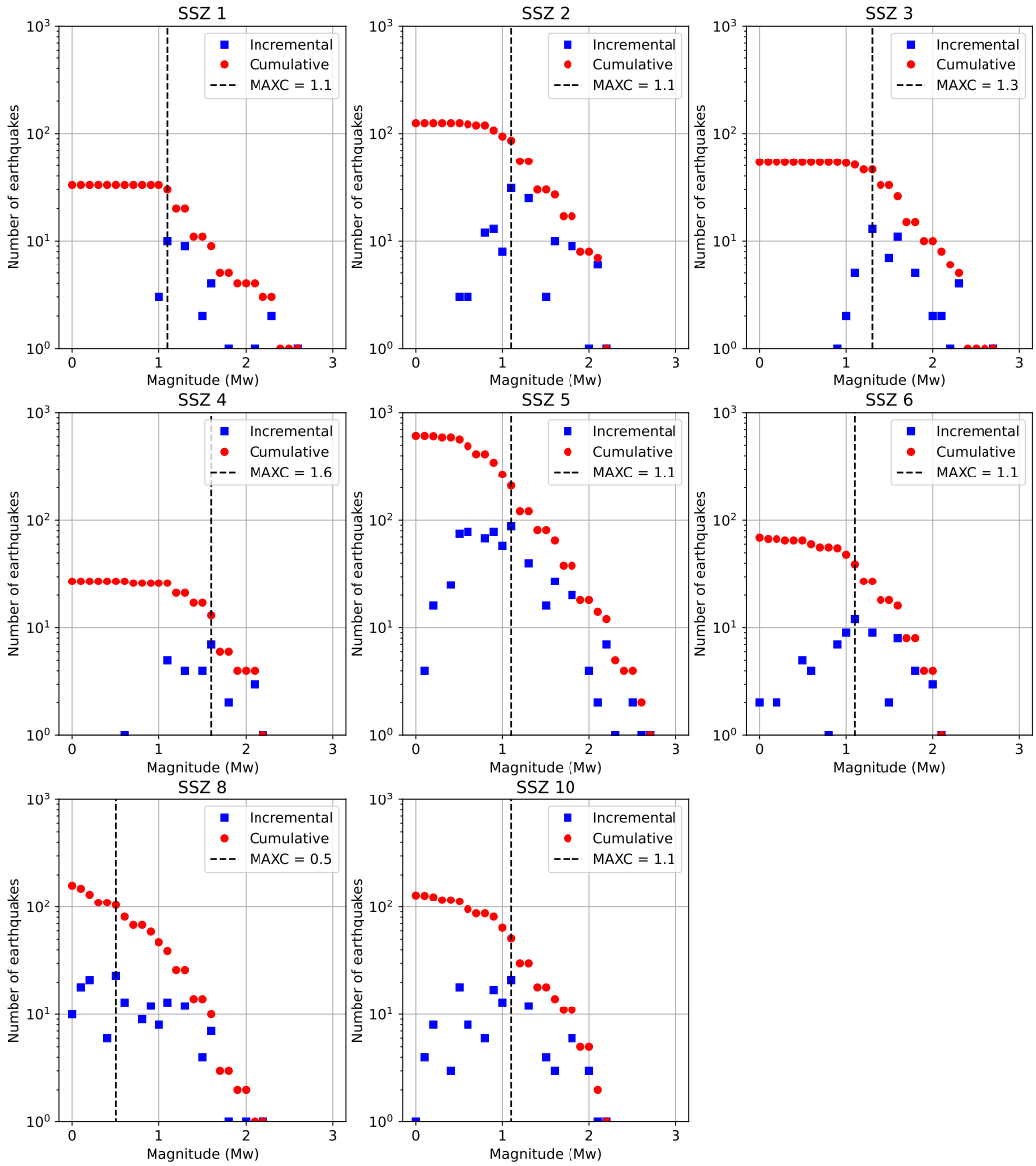


**Figure 4:** Cumulative and incremental FMD for the SSZs with the most recent ten years of data. Dashed vertical lines indicate the point of MAXC.

Because the following completeness evaluation and the GR parameter estimation is performed with a bin width of 0.5 Mw, to simplify the implementation, the minimum moment magnitude was set to either 0.5, 1.0 or 1.5. According to Tiira et al. [52], the nationwide threshold magnitude for complete reporting in Finland is approximately 0.9 on local magnitude scale. Based on this information and on the shapes of FMDs in Figure 4 it was decided to continue the analysis with a minimum magnitude of 1.0 Mw for SSZs 1, 2, 5, 6, 8 and 10. For SSZs 3 and 4, the minimum magnitude was set to 1.5 Mw.

As proposed by Stepp [20] the completeness of each magnitude bin was estimated by visually examining the standard deviation $\sigma_\lambda$ of the mean rate of occurrence $\lambda$ as a function of time period length $T$. Figure 5 shows the completeness analysis plots for individual source zones. The goal is to find the time period after which standard deviation significantly deviates from the expected behavior $\frac{1}{\sqrt{T}}$.

As an example consider the plot for SSZ 5 in Figure 5 which has the most observations and is the most clearly interpretable. For the smaller magnitude bins 1.0-1.5 Mw and 1.5-2.0 Mw, the standard deviation approximately follows the $\frac{1}{\sqrt{T}}$ behavior until $T = 25$. Thus the period of complete reporting, for these magnitude bins in SSZ 5, is estimated to begin from the start of the year 1997. The length of the complete time period seems to increase as magnitude increases. In SSZ 5, 2.0-2.5 Mw events can be seen completely reported during the most recent 60-year time period, 2.5-3.0 Mw events during the most recent 80-year time period and 3.0-3.5 Mw events during the most recent 140-year time period.

For larger magnitudes, with only a few recorded events that span across a long time period, the completeness estimation becomes challenging. For example, this can be seen with magnitude bin 3.5-4.0 Mw in SSZ 5, where the standard deviation does not distinctly stabilize during the time period covered by the catalog. Because the magnitude range observed in the study region is narrow to begin with, a significant amount of information could be lost if the magnitude bins, for which the completeness period cannot be unambiguously determined, were to be omitted from the hazard analysis.

To address the problem of increasing data sparsity as a function of magnitude, the completeness evaluation was conducted in parts. First the completeness of earthquakes with moment magnitudes smaller than 2 Mw were evaluated separately for each source zone. At moment magnitudes larger than 2 Mw, the data is already relatively sparse. Thus, at magnitudes 2.0-3.5 Mw the evaluation was conducted in four different groups. The groups used were [1 and 4], [2 and 3], [5] and [6, 8 and 10]. For magnitudes higher than 3.5 Mw, the analysis was conducted using the whole study region. Figure 6 shows the completeness analysis plot for the source zone groups and Figure 7 for the whole study region.

The results of this procedure are summarized in Table 4, by using Figure 5 to estimate the completeness of the smallest magnitude bins. The incompleteness of magnitude bin 1.0-1.5 Mw in SSZs 3 and 4 can also be seen in Figure 5, because even at short

time intervals, the standard deviation for this bin is smaller than the standard deviation for the next magnitude bin. Thus the previous assessment, that $m_c$ is equal to 1.5 Mw in SSZs 3 and 4, seems appropriate. Magnitudes 2.0-3.5 Mw were estimated in groups by examining Figure 6 and the completeness of earthquakes with magnitudes larger than 3.5 Mw were evaluated from Figure 7. As seen from Figure 7, even when data from the whole study region is used, $\sigma_\lambda$ does not stabilize and the completeness of magnitude bin 4.0-4.5 Mw cannot be reliably determined. Thus, the completeness period of magnitude bin 3.5-4.0 Mw was designated to all of the larger magnitude bins. The assumption, that the complete time period for the larger magnitude bin is at least as long as the complete period for the smaller magnitude bin, was used throughout the completeness evaluation.

The completeness periods were also evaluated solely with the data from individual SSZs. In this approach, if the completeness period of a magnitude bin could not be determined from Figure 5, it was decided to use the completeness period defined for the previous smaller magnitude bin. The results of this approach are summarized in Table A1 of Appendix A. The completeness periods defined with this approach are shorter and more conservative. This can be seen especially for SSZs 6 and 10. When the completeness is evaluated for larger magnitude with the SSZ group [6,8 and 10], SSZ 8, which has the most observations in that group, dominates the evaluation. However, conducting the assessment with individual SSZs, does not ensure better accuracy, because less data is used and the sensitivity to individual datapoints is increased.

**Table 4:** First year of completeness interval by magnitude bin for the SSZs. All of the completeness intervals start from the first day of the given year and end at the end of 2021. Different colors represent the grouping of sources used in the completeness analysis.

| | Magnitude Bin | | | | | |
|---|---|---|---|---|---|---|
| SSZ | 1.0-1.5 | 1.5-2.0 | 2.0-2.5 | 2.5-3.0 | 3.0-3.5 | 3.5- |
| 1 | 2007 | 1992 | 1962 | 1782 | 1742 | 1742 |
| 2 | 2002 | 1992 | 1962 | 1882 | 1882 | 1742 |
| 3 | - | 2002 | 1962 | 1882 | 1882 | 1742 |
| 4 | - | 2002 | 1962 | 1782 | 1742 | 1742 |
| 5 | 1997 | 1997 | 1962 | 1942 | 1882 | 1742 |
| 6 | 2012 | 2012 | 1882 | 1742 | 1742 | 1742 |
| 8 | 2012 | 2002 | 1882 | 1742 | 1742 | 1742 |
| 10 | 2007 | 2007 | 1882 | 1742 | 1742 | 1742 |

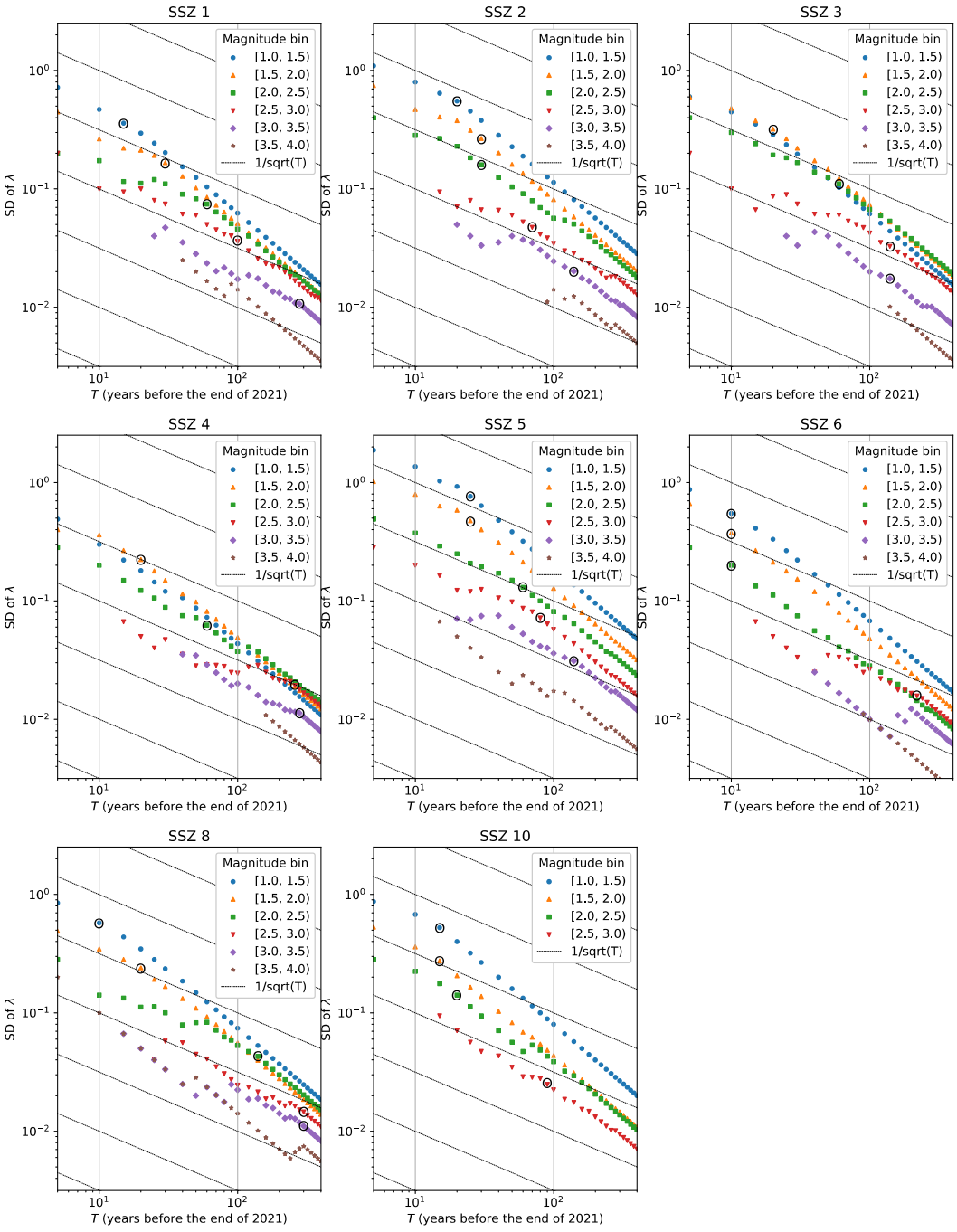


**Figure 5:** Stepp [20] completeness analysis plots for the individual SSZs. The standard deviation $\sigma_\lambda$ of the mean rate of occurrence $\lambda$, for each magnitude bin, is plotted as a function of time. Black dashed lines $\frac{1}{\sqrt{T}}$, with different scaling, indicate expected behavior of $\sigma_\lambda$ in a complete time period. The estimated completeness period length for the magnitude bin is indicated with a black circle.

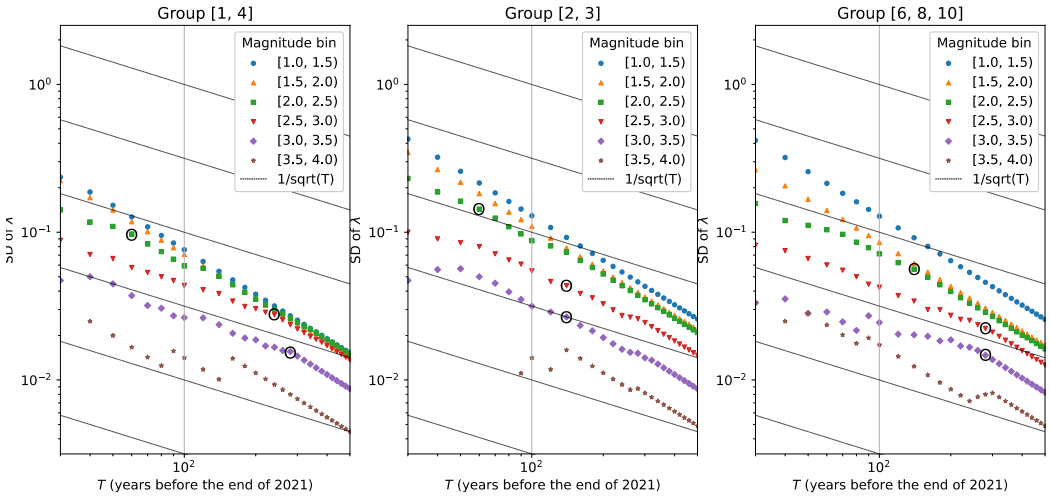


**Figure 6:** Stepp [20] completeness analysis plots for the SSZ groups. The estimated completeness period length is indicated with a black circle for the magnitude bins between 2.0-3.5 Mw.

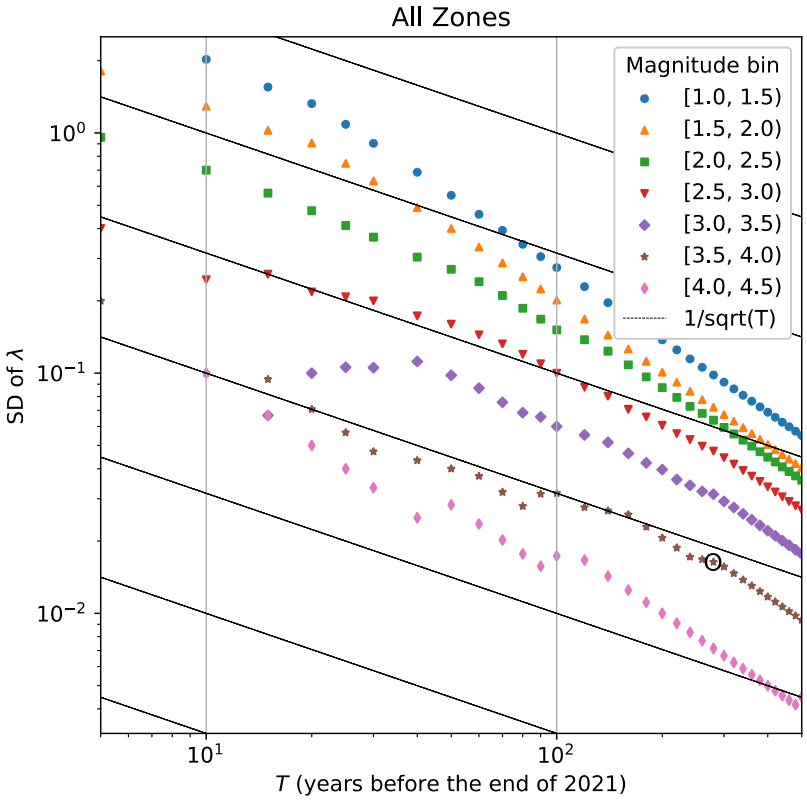


**Figure 7:** Stepp [20] completeness analysis plots for the whole region. The estimated completeness period length is indicated with a black circle for the magnitude bin 3.5-4.0 Mw.

## 4.2 Earthquake Recurrence

The completeness intervals defined in the previous Section 4.1 were used to estimate earthquake recurrence in the SSZs. First the completeness intervals defined with the SSZ grouping (Table 4) were used to filter out incompletely reported earthquakes from the catalog. The completeness intervals of SSZ 6 were applied to its sub-zones 6a, 6b and 6c. Table 5 shows the number of earthquakes by magnitude bin for each SSZ after the filtering.

**Table 5:** Number of earthquakes by magnitude bin and SSZ, after filtering out earthquakes outside the completeness intervals defined in Table 4.

| | Magnitude Bin | | | | | | |
|---|---|---|---|---|---|---|---|
| SSZ | 1.0-1.5 | 1.5-2.0 | 2.0-2.5 | 2.5-3.0 | 3.0-3.5 | 3.5-4.0 | 4.0-4.5 |
| 1 | 29 | 25 | 20 | 19 | 9 | 2 | 1 |
| 2 | 122 | 64 | 30 | 16 | 8 | 4 | 0 |
| 3 | - | 41 | 44 | 21 | 6 | 2 | 0 |
| 4 | - | 20 | 14 | 25 | 10 | 3 | 0 |
| 5 | 365 | 141 | 61 | 33 | 19 | 5 | 1 |
| 6 (whole) | 30 | 14 | 9 | 13 | 6 | 1 | 1 |
| 6a | 14 | 1 | 2 | 4 | 0 | 0 | 0 |
| 6b | 10 | 5 | 4 | 4 | 1 | 1 | 0 |
| 6c | 6 | 8 | 3 | 5 | 5 | 0 | 1 |
| 8 | 33 | 23 | 36 | 18 | 11 | 4 | 1 |
| 10 | 62 | 17 | 17 | 8 | 0 | 0 | 0 |

The recurrence for the SSZs were estimated from this data using both the LS and the MLE method presented in Section 3.3. The estimated recurrence curves are presented in Figure 8. The curves are plotted without any maximum magnitude truncation and until moment magnitude 5.75, after which it is assumed that $b = 2$. Figure 8 also shows the annual rates that are summed cumulative, starting from the largest magnitude bin. As the usual convention, these cumulative datapoints are presented at the lower bound of the magnitude bin. The corresponding recurrence parameters used as an input for the hazard calculations are in Table 6 for the LS and in Table 7 for the MLE. The recurrence parameters were also estimated with the completeness analysis results conducted without any SSZ grouping (Table A1), and the corresponding results are in Appendix A.

The estimated recurrence curves in Figures 8 and A1 show significant variation depending on whether the estimation was carried out with the LS or MLE method. Unlike the LS method, that weights each datapoint equally, the MLE estimation gives more significance to the lower magnitude bins containing more earthquake observations. Also, the recurrence curves estimated with the LS show an upward shift (i.e. larger estimate for the parameter $a$) compared to the curves estimated with the MLE. This shift is at least partly explained by the positioning of the datapoints in the LS method. With the LS method, used in this thesis and in the PSHA2021 [45], the

recurrence rates were estimated from datapoints such that the cumulative annual rates were placed at the center of the magnitude bin. Whereas the MLE method utilizes the non-cumulative datapoints, placed at the the center of the magnitude bin, and the underlying distribution to estimate the cumulative rate.

Another observation is that in most cases, the confidence interval estimates are much wider for the LS than for the MLE. Because the LS variance defined in Equation (14) measures the variability in the $y$-axis, rather than measuring how well the line fits the data, wider confidence intervals can be seen in SSZs in which the datapoints are aligned with a steeper slope, such as SSZ 10. Due to the longer completeness periods and updated data, compared to the PSHA2021 and to the sensitivity analysis thesis [5], more earthquake observations were utilized in the recurrence estimation of this thesis. This can be seen in a smaller uncertainty and narrower confidence intervals for the ML estimates. However, the increase in the earthquake observations is not reflected in a similar manner to the confidence intervals of the LS estimates.

**Table 6:** Recurrence parameters estimated with LS & Catalog completeness with SSZ groups (Table 4). $n_{\min}$ and its confidence bounds are defined for the minimum magnitude 4.5 Mw, used in the hazard calculations.

| SSZ | $b$ | $b_L$ | $b_U$ | $n_{\min}$ | $n_{\min,L}$ | $n_{\min,U}$ |
|---|---|---|---|---|---|---|
| 1 | 1.0038 | 0.7811 | 1.2264 | 0.0021183 | 0.0043117 | 0.0010407 |
| 2 | 1.1047 | 0.8168 | 1.3927 | 0.0023780 | 0.0073802 | 0.0007662 |
| 3 | 1.3025 | 0.8847 | 1.7204 | 0.0009556 | 0.0043205 | 0.0002113 |
| 4 | 1.0280 | 0.6986 | 1.3573 | 0.0020944 | 0.0068799 | 0.0006376 |
| 5 | 1.2442 | 0.9670 | 1.5213 | 0.0026765 | 0.0064835 | 0.0011049 |
| 6 | 1.0477 | 0.8126 | 1.2828 | 0.0013410 | 0.0028404 | 0.0006331 |
| 6a | 1.3483 | 0.7952 | 1.9013 | 0.0000403 | 0.0007972 | 0.0000020 |
| 6b | 1.0980 | 0.8071 | 1.3889 | 0.0003403 | 0.0010687 | 0.0001084 |
| 6c | 0.8889 | 0.6530 | 1.1247 | 0.0015480 | 0.0035732 | 0.0006707 |
| 8 | 1.0056 | 0.7822 | 1.2291 | 0.0024897 | 0.0050806 | 0.0012200 |
| 10 | 1.5531 | 0.9345 | 2.1718 | 0.0000544 | 0.0015332 | 0.0000019 |

**Table 7:** Recurrence parameters estimated with MLE & Catalog completeness with SSZ groups (Table 4). $n_{\min}$ and its confidence bounds are defined for the minimum magnitude 4.5 Mw, used in the hazard calculations.

| SSZ | $b$ | $b_L$ | $b_U$ | $n_{\min}$ | $n_{\min,L}$ | $n_{\min,U}$ |
|---|---|---|---|---|---|---|
| 1 | 0.9344 | 0.8402 | 1.0287 | 0.0018003 | 0.0034770 | 0.0009322 |
| 2 | 1.0976 | 1.0204 | 1.1747 | 0.0012884 | 0.0023140 | 0.0007173 |
| 3 | 1.1854 | 1.0558 | 1.3150 | 0.0008790 | 0.0019882 | 0.0003886 |
| 4 | 1.0000 | 0.8555 | 1.1445 | 0.0013871 | 0.0032616 | 0.0005899 |
| 5 | 1.0857 | 1.0356 | 1.1359 | 0.0034134 | 0.0050418 | 0.0023109 |
| 6 | 1.2160 | 1.0835 | 1.3485 | 0.0002051 | 0.0005154 | 0.0000816 |
| 6a | 1.5798 | 1.2819 | 1.8778 | 0.0000044 | 0.0000408 | 0.0000005 |
| 6b | 1.2527 | 1.0217 | 1.4837 | 0.0000540 | 0.0002725 | 0.0000107 |
| 6c | 0.9694 | 0.7688 | 1.1701 | 0.0003924 | 0.0014643 | 0.0001051 |
| 8 | 1.0426 | 0.9435 | 1.1417 | 0.0010199 | 0.0019881 | 0.0005232 |
| 10 | 1.5116 | 1.3731 | 1.6501 | 0.0000272 | 0.0000775 | 0.0000095 |

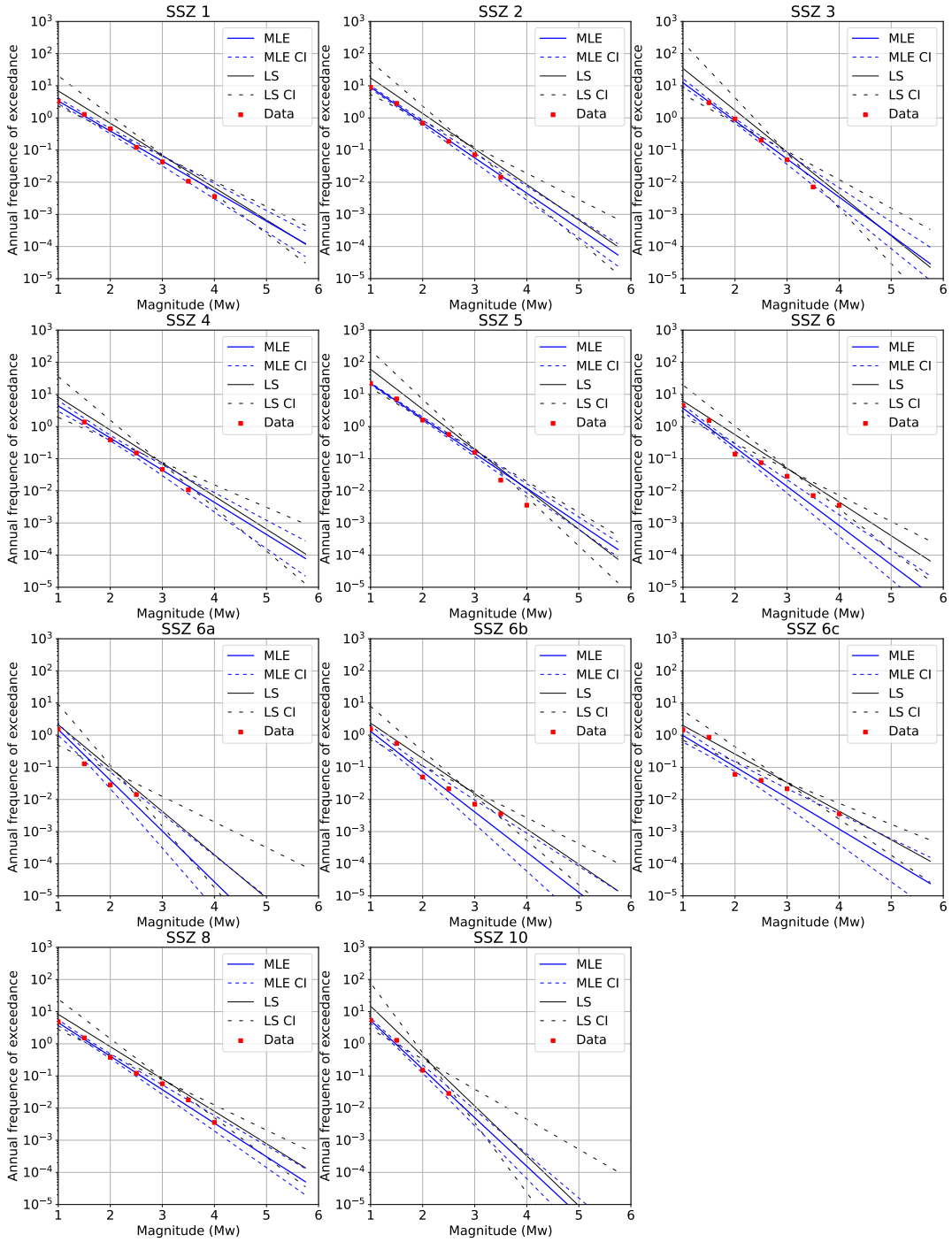


**Figure 8:** Recurrence curve means and confidence intervals (CI) calculated with LS and MLE, using the completeness intervals defined in Table 4. The cumulative datapoints are presented for the lower bound of the corresponding magnitude bin.

## 4.3 Hazard

First the sensitivity of the hazard estimates for the different completeness analysis and recurrence estimation approaches was studied. These different combinations were included in to the hazard model by using the logic tree shown in Figure 3, and the results are shown for Loviisa site in Section 4.3.2 and for Olkiluoto site in Section 4.3.3.

An examination of the hazard results showed that changing the parameters seismogenic thickness, fault plane dip or fault type did not have any impact on the hazard estimates. However, the results were affected by the shape of the focal depth distribution defined for each SSZ. This is an expected result, because the sources are modelled as areal sources and not as individual faults. The depth distribution is taken into account in the source-to-site distance $r$ in Equation (6).

### 4.3.1 Sensitivity to Modelling Decisions

Figure 9 shows the Loviisa mean 100 Hz hazard curves for the different completeness analysis and recurrence estimation combinations. The mean uniform hazard response spectra comparison at AFE $10^{-5}$ is in Figure 10. The corresponding results for Olkiluoto site are in Figures 11 and 12. The UHRS results at various AFE-levels and for all of the 4 modelling combinations are given in tabular form in Appendix B (Loviisa site) and in Appendix C (Olkiluoto site). The abbreviations w/ and w/o indicate whether the completeness analysis was conducted with or without the SSZ groups.

The hazard estimates decrease significantly when MLE is used for the recurrence parameters, which is inline with the sensitivity analysis thesis [5]. Also, the completeness evaluation has a major impact on the estimates. As the more conservative completeness periods are used, i.e. completeness periods evaluated with the data from individual SSZ, the hazard estimates increase with both the MLE and LS.

SSZ 10, which is the host zone for Loviisa site, has observations from a narrower magnitude range than the Olkiluoto host zone SSZ 6. Also, the difference between the two completeness results is more significant for the SSZ 10 than it is for the SSZ 6. This is reflected in the hazard estimates, as the estimates for the Loviisa site (Figures 9 and 10) are more sensitive to the different modelling decisions, than the estimates for the Olkiluoto site (Figures 11 and 12).

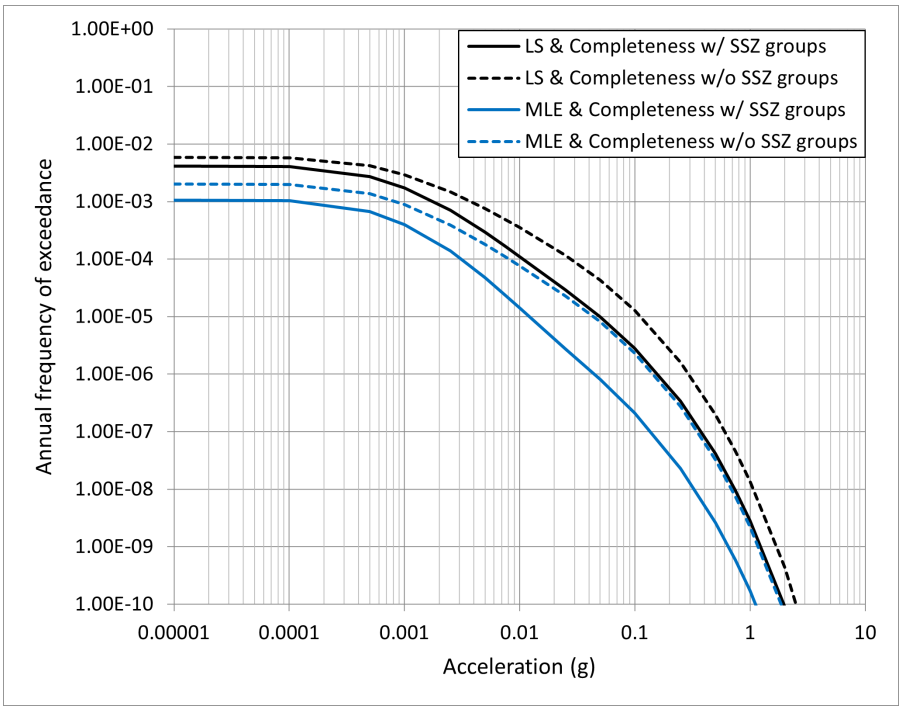


**Figure 9:** Loviisa mean hazard curve comparison at frequency of 100 Hz.

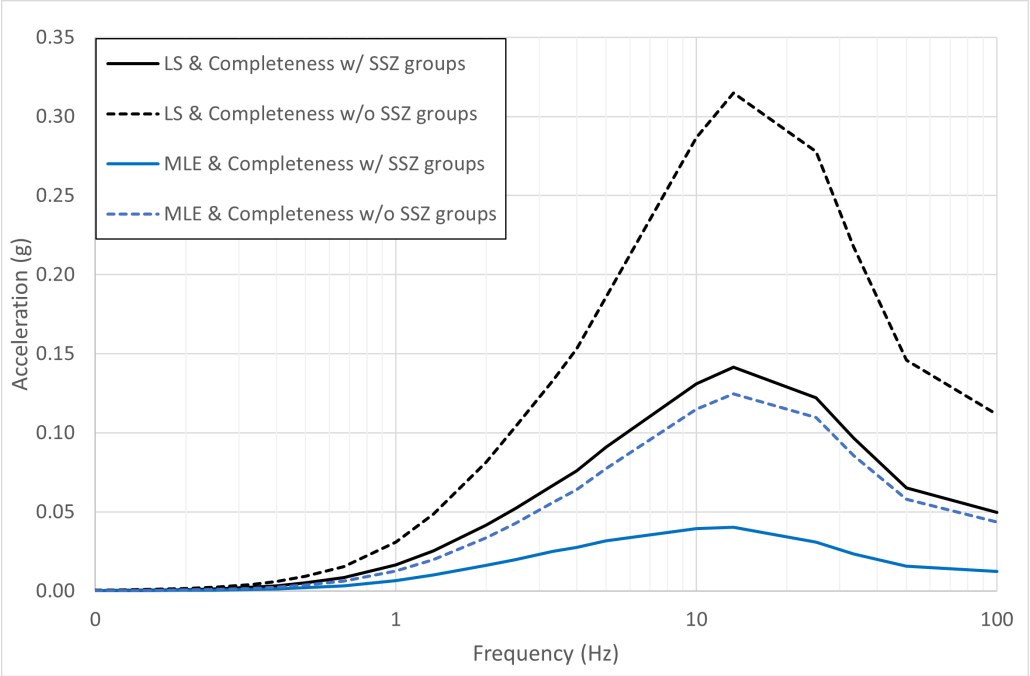


**Figure 10:** UHRS comparison at $10^{-5}$ mean AFE for Loviisa site.

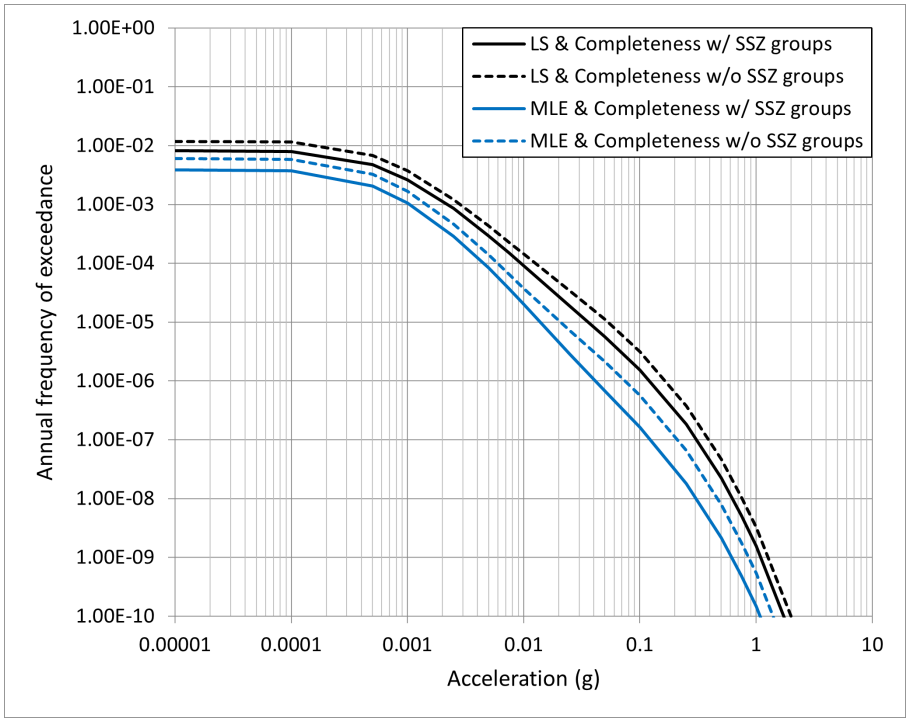


**Figure 11:** Olkiluoto mean hazard curve comparison at frequency of 100 Hz.

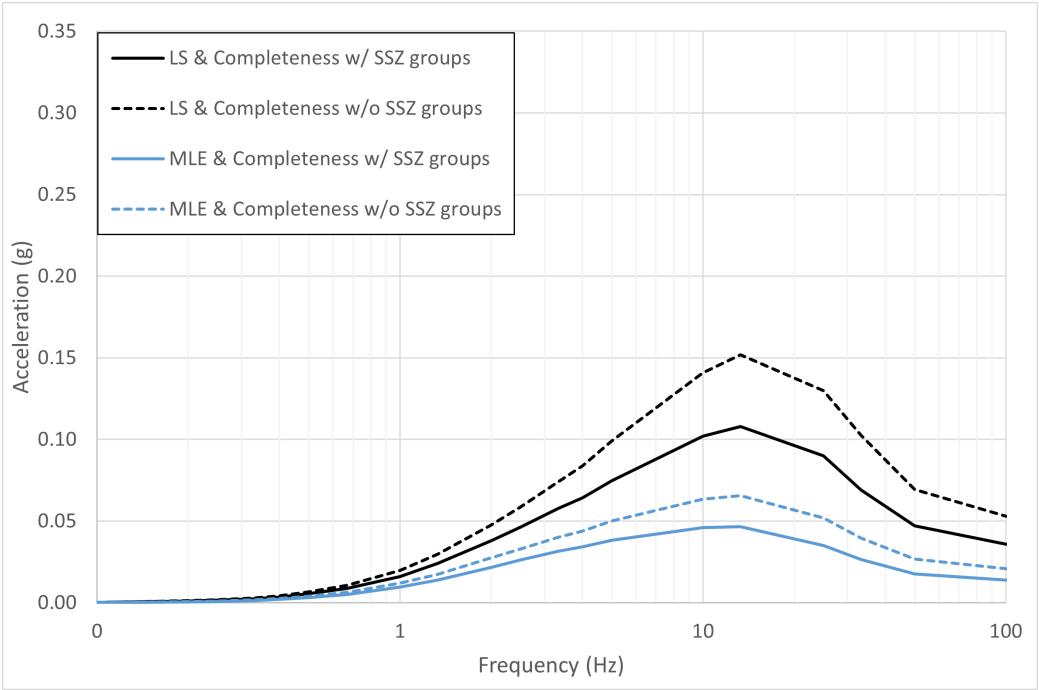


**Figure 12:** UHRS comparison at $10^{-5}$ mean AFE for Olkiluoto site.

### 4.3.2 Loviisa Hazard

The hazard calculations were performed with the extended logic tree shown in Figure 3. Figure 13 shows the mean hazard curves by SSZ and the total mean for Loviisa site at four different frequencies. SSZs 6, 8 and 11 have the largest contribution to the hazard at small accelerations. The hazard contribution of the host zone SSZ 10 increases as larger accelerations are considered. For example at AFE of $10^{-5}$ the total hazard estimate is almost completely covered by the SSZ 10.

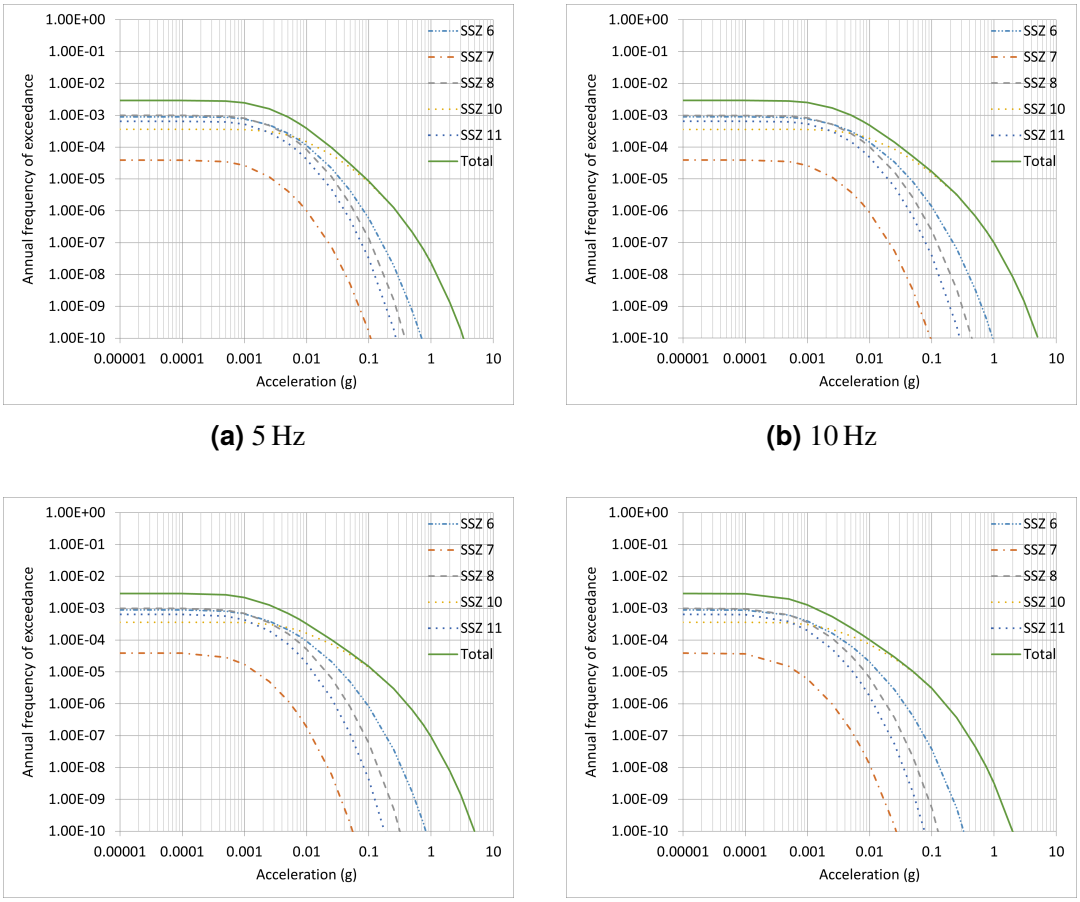


**(a)** 5 Hz

**(b)** 10 Hz

**(c)** 25 Hz

**(d)** 100 Hz

**Figure 13:** Loviisa mean hazard curves by SSZ and the total mean at different frequencies.

In addition to the mean hazard, the estimated 0.05-, 0.16-, 0.5-, 0.84- and 0.95-fractiles are shown in Figure 14. The 0.5-fractile (i.e. the median) values are smaller than the mean values at each frequency. At larger accelerations even the 0.84-fractile is exceeded by the mean.

The resulting mean UHRS for Loviisa at AFEs from $10^{-4}$ to $10^{-6}$ are in Figure 15. The corresponding results from the PSHA2021 are shown as dashed lines. The results show a decrease in hazard at each AFE and frequency. The relative difference in results is the largest at smallest frequencies and increases as the AFE increases. The shapes of the UHRS are similar to the shapes of the PSHA2021 UHRS. From the frequencies

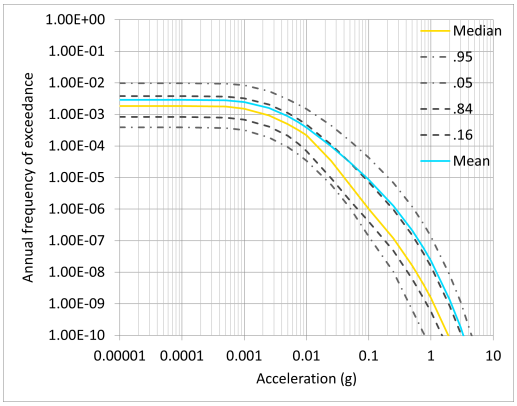


**(a)** 5 Hz

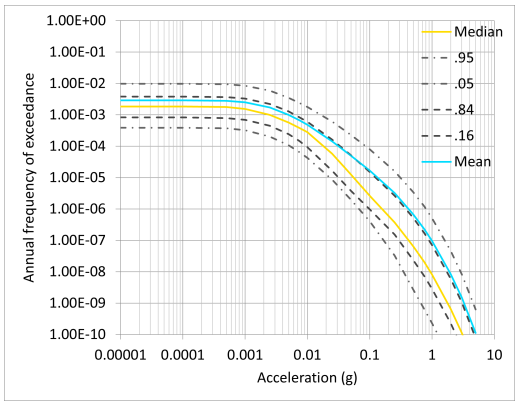


**(b)** 10 Hz

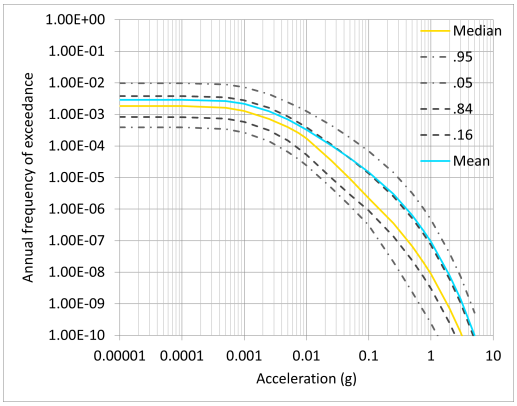


**(c)** 25 Hz

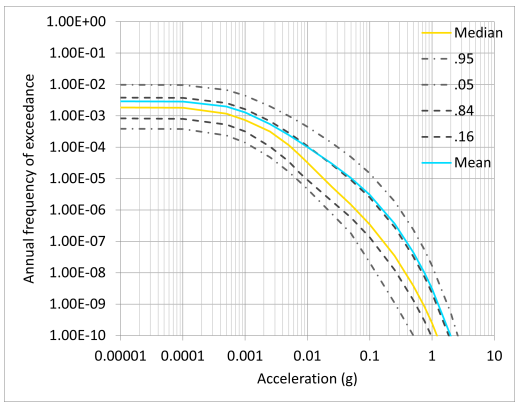


**(d)** 100 Hz

**Figure 14:** Loviisa hazard curves at different frequencies.

considered, the UHRS peaks at the frequency 13.33 Hz. The true peak seems to lie between the frequencies 13.33 Hz and 25 Hz. The UHRS values at different AFEs are tabulated in Table 8.

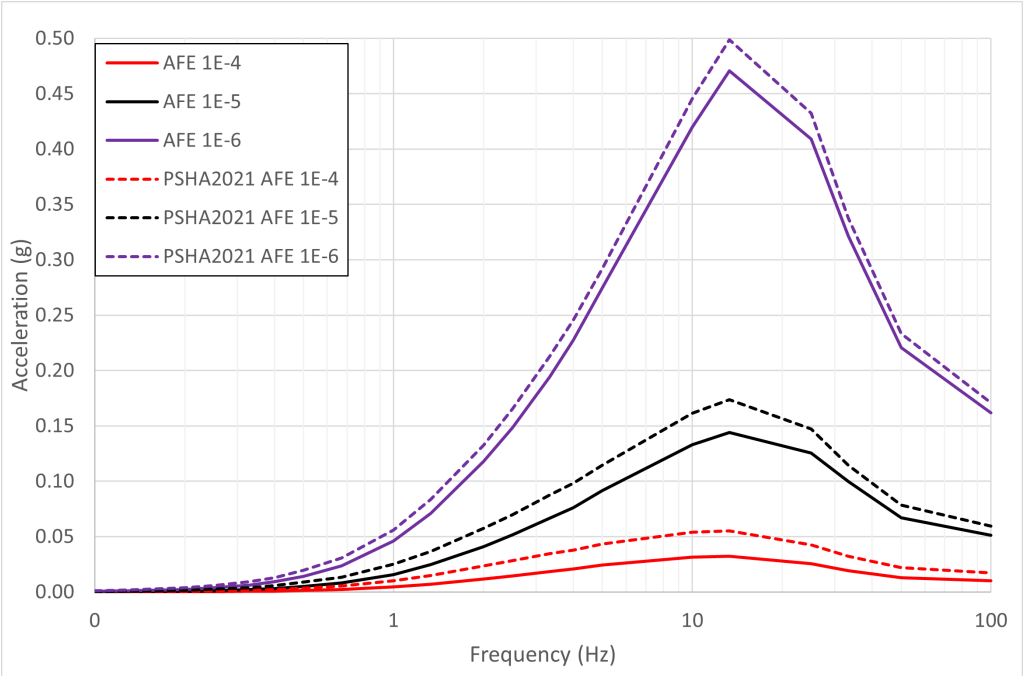


**Figure 15:** Loviisa mean UHRS at different AFEs. The PSHA2021 results are shown as dashed lines for comparison.

**Table 8:** Loviisa mean uniform hazard response spectra.

| Frequency (Hz) | SA at mean AFE $10^{-3}$ (g) | SA at mean AFE $10^{-4}$ (g) | SA at mean AFE $10^{-5}$ (g) | SA at mean AFE $10^{-6}$ (g) | SA at mean AFE $10^{-7}$ (g) | SA at mean AFE $10^{-8}$ (g) |
|---|---|---|---|---|---|---|
| 0.10 | 0.00000 | 0.00004 | 0.00018 | 0.00059 | 0.00155 | 0.00355 |
| 0.13 | 0.00000 | 0.00007 | 0.00032 | 0.00106 | 0.00276 | 0.00628 |
| 0.20 | 0.00002 | 0.00018 | 0.00076 | 0.00234 | 0.00592 | 0.01295 |
| 0.25 | 0.00003 | 0.00029 | 0.00121 | 0.00363 | 0.00921 | 0.02006 |
| 0.33 | 0.00006 | 0.00053 | 0.00207 | 0.00633 | 0.01591 | 0.03558 |
| 0.40 | 0.00010 | 0.00078 | 0.00304 | 0.00914 | 0.02306 | 0.05104 |
| 0.50 | 0.00016 | 0.00126 | 0.00486 | 0.01415 | 0.03572 | 0.07765 |
| 0.67 | 0.00027 | 0.00214 | 0.00802 | 0.02355 | 0.05886 | 0.12498 |
| 1.00 | 0.00067 | 0.00444 | 0.01569 | 0.04612 | 0.11282 | 0.23753 |
| 1.33 | 0.00112 | 0.00701 | 0.02457 | 0.07092 | 0.17074 | 0.35360 |
| 2.00 | 0.00201 | 0.01176 | 0.04091 | 0.11796 | 0.28309 | 0.56895 |
| 2.50 | 0.00263 | 0.01452 | 0.05158 | 0.14817 | 0.35416 | 0.71322 |
| 3.33 | 0.00334 | 0.01855 | 0.06652 | 0.19417 | 0.46096 | 0.90625 |
| 4.00 | 0.00370 | 0.02078 | 0.07595 | 0.22717 | 0.53576 | 1.04552 |
| 5.00 | 0.00429 | 0.02448 | 0.09147 | 0.27427 | 0.63939 | 1.22490 |
| 10.00 | 0.00502 | 0.03160 | 0.13307 | 0.41962 | 0.98837 | 1.90134 |
| 13.33 | 0.00478 | 0.03241 | 0.14416 | 0.47064 | 1.10179 | 2.15969 |
| 25.00 | 0.00327 | 0.02559 | 0.12524 | 0.40915 | 0.96950 | 1.86527 |
| 33.33 | 0.00252 | 0.01932 | 0.09991 | 0.32152 | 0.76461 | 1.44546 |
| 50.00 | 0.00162 | 0.01301 | 0.06699 | 0.22072 | 0.52230 | 1.00842 |
| 100.00 | 0.00130 | 0.01008 | 0.05112 | 0.16196 | 0.38445 | 0.75468 |

### 4.3.3 Olkiluoto Hazard

The corresponding results for Olkiluoto site are in this section. As can be seen from Figure 16, at smallest accelerations the most contributing zones are SSZs 2 and 3, but the contribution rapidly decreases as larger accelerations are considered. This is logical, as the SSZs 2 and 3 are more seismically active than the zones nearby Olkiluoto NPP, but given the larger distance, the ground motions from the SSZs 2 and 3 are affected by greater attenuation. As in the Loviisa case, at larger accelerations the hazard is dominated by the NPPs host zone.

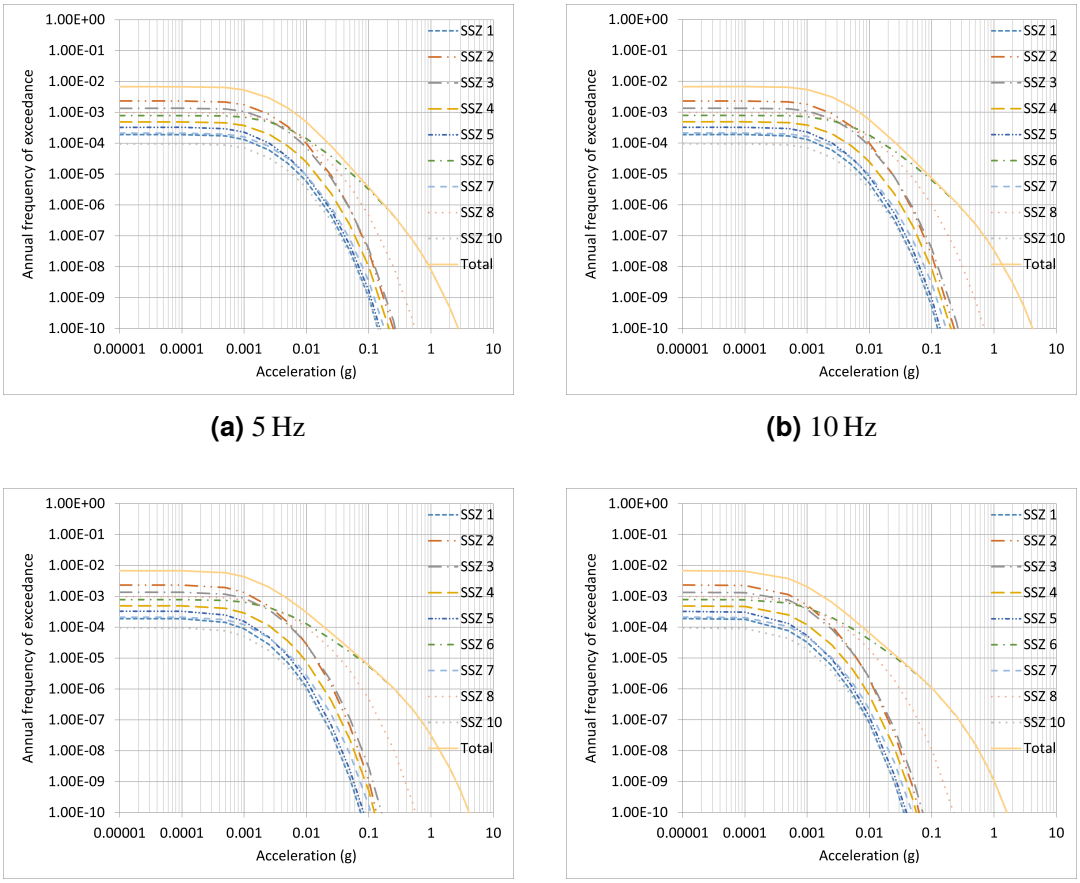


**(a)** 5 Hz

**(b)** 10 Hz

**(c)** 25 Hz

**(d)** 100 Hz

**Figure 16:** Olkiluoto mean hazard curves by SSZ and the total mean at different frequencies.

The estimated 0.05-, 0.16-, 0.5-, 0.84- and 0.95-fractiles and the mean hazard at different frequencies are shown in Figure 17. Compared to the Loviisa site, the fractals are not as widely spread out. As in the Loviisa site, the mean is higher than the median but the difference between them is not as large.

The mean UHRS for Olkiluoto site at AFEs from $10^{-4}$ to $10^{-6}$ are in Figure 18. The UHRS results are given in tabulated form in Table 9. The shapes of the spectra are similar to the Loviisa UHRS, peaking at 13.33 Hz from the frequencies considered.

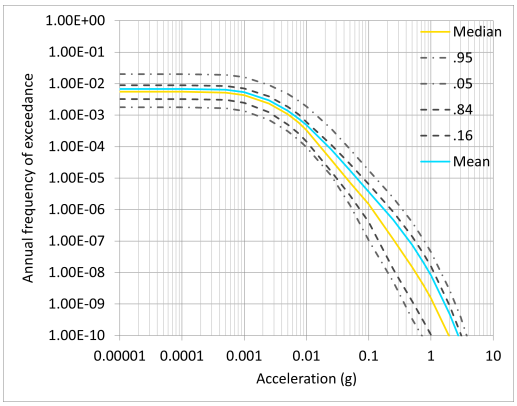


**(a)** 5 Hz

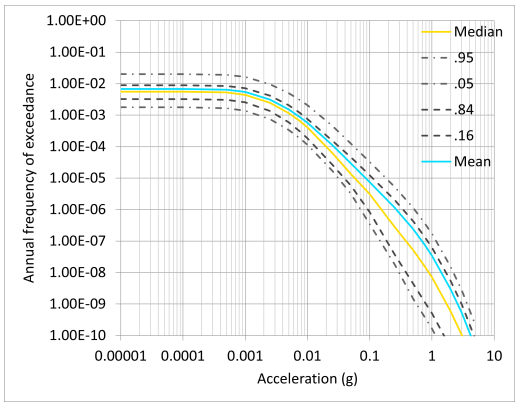


**(b)** 10 Hz

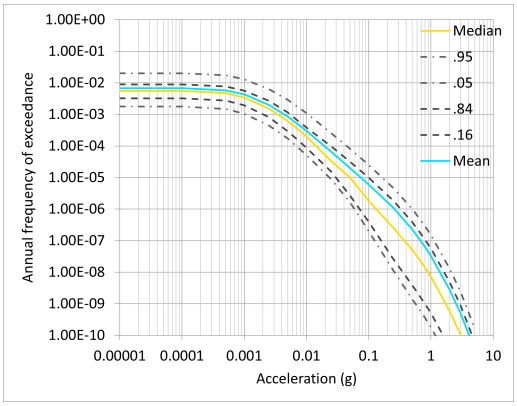


**(c)** 25 Hz

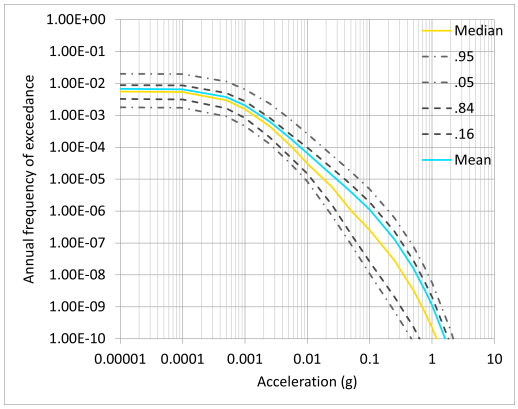


**(d)** 100 Hz

**Figure 17:** Olkiluoto hazard curves at different frequencies.

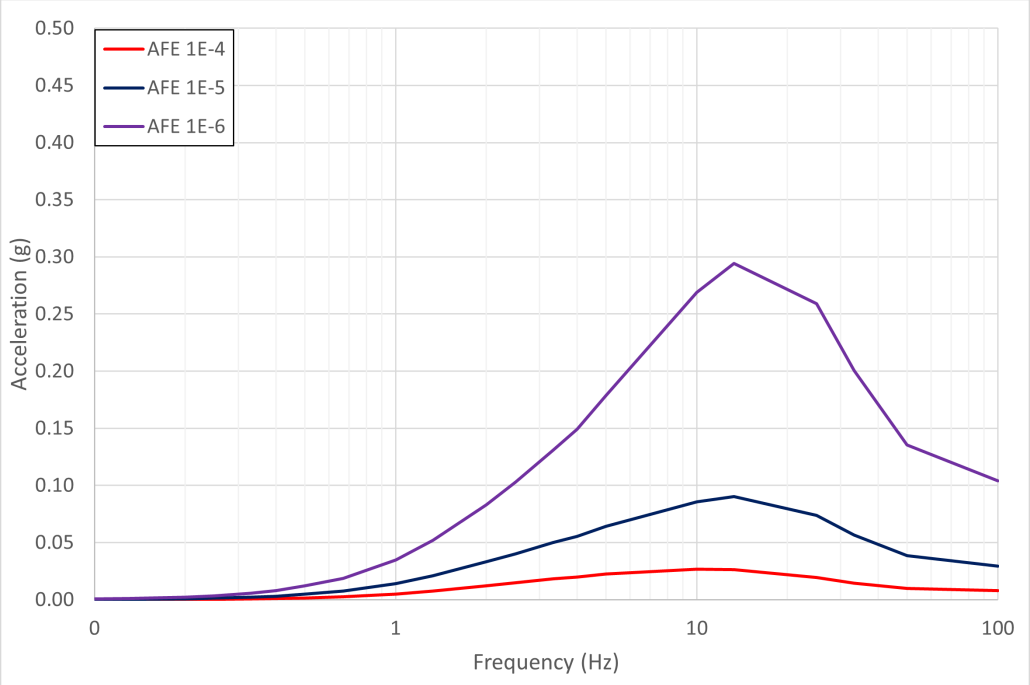


**Figure 18:** Olkiluoto mean UHRS at different AFEs.

**Table 9:** Olkiluoto mean uniform hazard response spectra.

| Frequency (Hz) | SA at mean AFE $10^{-3}$ (g) | SA at mean AFE $10^{-4}$ (g) | SA at mean AFE $10^{-5}$ (g) | SA at mean AFE $10^{-6}$ (g) | SA at mean AFE $10^{-7}$ (g) | SA at mean AFE $10^{-8}$ (g) |
|---|---|---|---|---|---|---|
| 0.10 | 0.00000 | 0.00005 | 0.00020 | 0.00060 | 0.00138 | 0.00284 |
| 0.13 | 0.00002 | 0.00010 | 0.00036 | 0.00104 | 0.00240 | 0.00489 |
| 0.20 | 0.00004 | 0.00023 | 0.00082 | 0.00218 | 0.00492 | 0.01005 |
| 0.25 | 0.00007 | 0.00038 | 0.00127 | 0.00332 | 0.00748 | 0.01524 |
| 0.33 | 0.00012 | 0.00065 | 0.00212 | 0.00555 | 0.01251 | 0.02659 |
| 0.40 | 0.00018 | 0.00097 | 0.00305 | 0.00786 | 0.01758 | 0.03747 |
| 0.50 | 0.00029 | 0.00152 | 0.00480 | 0.01197 | 0.02715 | 0.05762 |
| 0.67 | 0.00054 | 0.00255 | 0.00760 | 0.01866 | 0.04313 | 0.09353 |
| 1.00 | 0.00115 | 0.00505 | 0.01407 | 0.03472 | 0.08088 | 0.17207 |
| 1.33 | 0.00182 | 0.00768 | 0.02099 | 0.05189 | 0.12183 | 0.26542 |
| 2.00 | 0.00321 | 0.01219 | 0.03318 | 0.08299 | 0.19846 | 0.42266 |
| 2.50 | 0.00399 | 0.01464 | 0.04020 | 0.10287 | 0.25293 | 0.53436 |
| 3.33 | 0.00512 | 0.01806 | 0.05004 | 0.13083 | 0.32192 | 0.68181 |
| 4.00 | 0.00557 | 0.01976 | 0.05541 | 0.14916 | 0.37217 | 0.79085 |
| 5.00 | 0.00626 | 0.02247 | 0.06412 | 0.17842 | 0.44994 | 0.94109 |
| 10.00 | 0.00682 | 0.02651 | 0.08561 | 0.26898 | 0.69371 | 1.41770 |
| 13.33 | 0.00646 | 0.02634 | 0.09003 | 0.29437 | 0.77849 | 1.60864 |
| 25.00 | 0.00435 | 0.01925 | 0.07385 | 0.25900 | 0.67877 | 1.39186 |
| 33.33 | 0.00325 | 0.01451 | 0.05651 | 0.20033 | 0.53590 | 1.10569 |
| 50.00 | 0.00219 | 0.00980 | 0.03836 | 0.13555 | 0.36091 | 0.76435 |
| 100.00 | 0.00176 | 0.00776 | 0.02936 | 0.10406 | 0.27297 | 0.56871 |

# 5 Discussion and Conclusions

In this thesis, the seismic hazard for the NPP sites in Finland was studied utilizing the PSHA methodology. The analysis was largely based on a earlier PSHA study (PSHA2021) [4] and related reports [5, 6]. The new earthquake catalog [7] was used, and the completeness of it for PSHA purposes was investigated. Also, the effect of using MLE instead of LS method in the GR parameter estimation was studied. Finally, efforts were made to incorporate the uncertainties associated with the completeness evaluation and the GR parameter estimation method into the PSHA by utilizing the logic tree approach.

The completeness evaluation of the earthquake catalog is a challenging yet important part of the analysis. In the PSHA2021, it was assumed that the completeness periods do not vary across different SSZs in the study region. In this thesis, it was found that the completeness of the catalog has regional differences leading to a more detailed analysis. However, as the geographic detail of the analysis is increased, the sparsity of data becomes problematic especially at larger magnitudes. Thus, it was decided not to only evaluate the catalog completeness in individual SSZs, but to also conduct an analysis in which the completeness of larger earthquakes was evaluated with groups of SSZs. The GR parameters and the hazard show a high sensitivity to the completeness evaluation.

The Stepp method [20], which was used to evaluate the magnitude dependent completeness periods, relies heavily on the visual interpretation of the analyst, and requires the binning of magnitudes. In this thesis the completeness was evaluated with a bin width of 0.5 Mw. If the bins are made smaller, the amount of data in each bin would be insufficient for a reliable analysis. Further investigation could be made to evaluate the completeness such that the analysis would not rely as heavily on the judgement of the analyst, and would enable the completeness assessment with an accuracy of 0.1 Mw. With a smaller bin width, the minimum magnitude used in the recurrence estimation could be defined more precisely.

It should be noted that the catalog used in this work did not undergo the same processing steps as the PSHA2021 catalog. Slate [4] revised the magnitude scale homogenization made by UH, whereas in this work the homogenized magnitudes provided by UH were accepted as such. However, during the PSHA2021 study it was pointed out that the homogenized magnitude revision has only a moderate impact on the hazard estimates. Also, different declustering methods were used as the Reasenberg method [17] was utilized in the PSHA2021.

After the declustering, the earthquakes in the catalog should be temporally independent on each other. However, some distinguishable peaks in the yearly earthquake observations were noticed in the declustered catalog of Loviisa NPP host zone, with one occurring in the year 2011. The events in the SSZ 10 present a challenge for declustering, because they exhibit swarm-like behaviour, where a distinct mainshock is not clearly distinguishable from a long series of small events [38]. Different declustering methods and magnitude scale conversions were not studied in this thesis,

yet they are a major part of PSHA because they affect the completeness evaluation, the GR parameters and the resulting hazard.

Compared to the PSHA2021, the earthquake catalog used in this work contained 7 years of new earthquake observations. Also, the completeness evaluations of the catalog resulted in a significantly longer completeness periods than in the PSHA2021. Therefore a lot more events were could be utilized for the earthquake recurrence estimation of this thesis. The complete catalog in the PSHA2021 contained 361 events, whereas in this thesis the corresponding catalog contained 1464 or 1429 events depending, whether the completeness was evaluated with or without the SSZ groups. Thus, the impact of an individual earthquake observation on the resulting hazard estimates has been notably reduced.

Using the MLE instead of the LS method used in the PSHA2021, resulted in a reduced hazard estimates for both NPP sites. The MLE method used in this work was derived by Visakorpi in the Master's thesis [5] and verified by Heikkilä in the special assignment [6]. A more commonly used method such as the MLE of Weichert [28] was not applied as it does not take into account the correlation between the GR parameters. However, according to [53], the often ignored correlation has a rather small and reducing impact on the hazard estimates. A smaller bin width, and thus a greater amount of datapoints, would make the LS estimates closer to the ML estimates. This was also concluded in [6], but the use of smaller bin width would still require the reassessment of the catalog completeness, as discussed earlier in this section.

As multiple sources e.g. [18, 29, 30] argue against the use LS in the GR parameter estimation, the rationale behind its use in the previous PSHA is unclear. Moreover, using the LS method such that the cumulative rates are placed at the center of the magnitude bin, results in more conservative recurrence estimates. Nonetheless, the LS was included into the final logic tree of this work. The replacement of the LS with the MLE method would require a verification that the new method is compatible with the modified HAZ45-software. Also, the novel method of assigning $b = 2$ for the larger magnitudes was not studied in this thesis and requires further justifications. The final logic tree weights were determined based on the confidence on each model but should be reassessed, for instance, when new information regarding the recurrence estimation method is obtained.

The modified computer program HAZ45, proposed some technical challenges for the analysis. The varying $b$-value approach in the recurrence model and the modified NGA-East GMPEs are hardcoded into the HAZ45 source code. Thus, it was not possible to examine how these modifications were implemented in the PSHA2021. Furthermore, due to this, the GMPE logic tree could not be used in the fractile estimation. In the future, it could be beneficial to conduct the calculations with another PSHA software. One option could be the OpenQuake software, which in addition to the hazard calculations, provides tools to examine the catalog completeness and estimate the recurrence parameters. Also, to mitigate the chance of errors, it would be useful to be able to analyse the results within the software without the need for external tools such as Excel.

# References


[1] Radiation and nuclear safety authority (STUK), “Provisions for internal and external hazards at a nuclear facility (YVL B.7).” (2019). [Online]. Available: https://www.stuklex.fi/en/ohje/YVLB-7 (visited on 28/09/2023).

[2] Burck, S., Holmberg, J. E., Lahtinen, M., Okko, O., Sandberg, J. and Välikangas, P. "Sensitivity study of seismic hazard prediction in Finland (SENSEI)" (2023).

[3] Baker, J. W. "Probabilistic seismic hazard analysis". *White Paper Version* 2.0 (2013), pp. 1-79.

[4] Slate Geotechnical Consultants, Inc. "Finland probabilistic seismic hazard analysis" (2021). LO1-T84252-00016Liite1.

[5] Visakorpi, V. “Sensitivity analysis of a seismic hazard assessment for a Finnish nuclear power plant”. Master’s thesis. Aalto University, School of Science. Espoo, Finland (2022).

[6] Heikkilä, L. "Verification and sensitivity analysis of maximum likelihood estimation for loviisa NPP seismic hazard". Special assignment. Aalto University, School of Science. Espoo, Finland (2023).

[7] University of Helsinki, Institute of Seismology. Earthquake catalog (2023). [Unpublished Excel spreadsheet].

[8] Cornell, C. A. “Engineering seismic risk analysis”. *Bulletin of the Seismological Society of America* 58.5 (1968), pp. 1583–1606.

[9] McGuire, R. K. "Probabilistic seismic hazard analysis: Early history". *Earthquake Engineering & Structural Dynamics* 37.3 (2008), pp. 329-338.

[10] Mulargia, F., Stark, P. B. and Geller, R. J. "Why is probabilistic seismic hazard analysis (PSHA) still used?". *Physics of the Earth and Planetary Interiors* 264 (2017), pp. 63-75.

[11] Puteri, D. M., Affandi, A. K., Sailah, S., Hudayat, N. and Zawawi, M. K. "Analysis of peak ground acceleration (PGA) using the probabilistic seismic hazard analysis (PSHA) method for Bengkulu earthquake of 1900–2017 period". *Journal of Physics: Conference Series* 1282.1 (2019), pp. 1-11.

[12] de Almeida, A. A. D., Assumpção, M., Bommer, J. J., Drouet, S., Riccomini, C. and Prates, C. L. "Probabilistic seismic hazard analysis for a nuclear power plant site in southeast Brazil". *Journal of Seismology* 23 (2019), pp. 1-23.

[13] Ansari, A., Zahoor, F., Rao, K. S. and Jain, A. K. "Seismic hazard assessment studies based on deterministic and probabilistic approaches for the Jammu region, NW Himalayas". *Arabian Journal of Geosciences* 15.11 (2022), pp. 1-26.

[14] Hanks, T. C. and Kanamori, H. "A moment magnitude scale". *Journal of Geophysical Research: Solid Earth* 84.B5 (1979), pp. 2348-2350.

[15] Cornell, C. A. and Winterstein, S. R. "Temporal and magnitude dependence in earthquake recurrence models". *Bulletin of the Seismological Society of America* 78.4 (1988), pp. 1522-1537.

[16] Gardner, J. K. and Knopoff, L. "Is the sequence of earthquakes in Southern California, with aftershocks removed, Poissonian?". *Bulletin of the Seismological Society of America* 64.5 (1974), pp. 1363-1367.

[17] Reasenberg, P. "Second-order moment of central California seismicity, 1969–1982". *Journal of Geophysical Research: Solid Earth* 90.B7 (1985), pp. 5479-5495.

[18] International Atomic Energy Agency (IAEA). "Diffuse seismicity in seismic hazard assessment for site evaluation of nuclear installations" *Safety Reports Series* 89 (2016).

[19] Tinti S. and Mulargia F. "Completeness analysis of a seismic catalog". *Annales Geophysicae* 3 (1985), pp. 407–414.

[20] Stepp, J. C. "Analysis of completeness of the earthquake sample in the Puget Sound area and its effect on statistical estimates of earthquake hazard". *Proceedings of the International Conference on Microzonation, Seattle* 2 (1972), pp. 897-910.

[21] Wyss, M., Schorlemmer, D. and Wiemer, S. (2000). "Mapping asperities by minima of local recurrence time: San Jacinto-Elsinore fault zones". *Journal of Geophysical Research: Solid Earth* 105.B4 (2000), pp.7829-7844.

[22] Wiemer, S. and Wyss, M. "Minimum magnitude of completeness in earthquake catalogs: Examples from Alaska, the western United States, and Japan". *Bulletin of the Seismological Society of America* 90.4 (2000), pp.859-869.

[23] Gutenberg, B. and Richter, C. F. "Frequency of earthquakes in California". *Bulletin of the Seismological Society of America* 34.4 (1944), pp. 185–188.

[24] McGuire, R. K. "Seismic hazard and risk analysis". Earthquake Engineering Research Institute (2004).

[25] Wells, D. L. and Coppersmith, K. J. "New empirical relationships among magnitude, rupture length, rupture width, rupture area, and surface displacement". *Bulletin of the Seismological Society of America* 84.4 (1994), pp. 974-1002.

[26] Kijko, A. "Estimation of the maximum earthquake magnitude, m max". *Pure and Applied Geophysics* 161 (2004), pp. 1655-1681.

[27] Aki, K. "Maximum likelihood estimate of b in the formula log N=a-bM and its confidence limits". *Bulletin of Earthquake Research Institute* 43 (1965), pp. 237–239.

[28] Weichert, D. H. "Estimation of the earthquake recurrence parameters for unequal observation periods for different magnitudes". *Bulletin of the Seismological Society of America* 70.4 (1980), pp. 1337-1346.

[29] Stromeyer, D. and Grünthal, G. "Capturing the uncertainty of seismic activity rates in probabilistic seismic hazard assessments". *Bulletin of the Seismological Society of America* 105.2A (2015), pp. 580-589.

[30] Sandri, L. and Marzocchi W. "A technical note on the bias in the estimation of the b-value and its uncertainty through the least squares technique". *Annals of Geophysics* 50.3 (2017), pp. 329–339.

[31] Stewart, J. P. et al. "Selection of ground motion prediction equations for the global earthquake model". *Earthquake Spectra* 31.1 (2015), pp. 19-45.

[32] Douglas, J. "Ground motion prediction equations (1964-2021)". [Online]. Available: http://www.gmpe.org.uk/gmpereport2014.pdf (visited on 06/02/2024).

[33] Bommer, J. J. and Crowley, H. "The purpose and definition of the minimum magnitude limit in PSHA calculations". *Seismological Research Letters* 88.4 (2017), pp. 1097-1106.

[34] Bommer, J. J. and Akkar, S. "Consistent source-to-site distance metrics in ground-motion prediction equations and seismic source models for PSHA". *Earthquake Spectra* 28.1 (2012), pp. 1-15.

[35] Bommer, J. J. and Scherbaum, F. "The use and misuse of logic trees in probabilistic seismic hazard analysis". *Earthquake Spectra* 24.4 (2008), pp. 997-1009.

[36] Kulkarni, R. B., Youngs, R. R. and Coppersmith, K. J. "Assessment of confidence intervals for results of seismic hazard analysis". In *Proceedings, Eighth World Conference on Earthquake Engineering* vol. 1 (1984), pp. 263–270.

[37] Abrahamson, N. HAZ45.3 (2023). [Online]. Available: https://github.com/abrahamson/HAZ (visited on 16/04/2024).

[38] Korja, A. et al. "Seismic source areas in central Fennoscandia". Institute of Seismology, Report S-64 (2016).

[39] Electric Power Research Institute (EPRI), Johnston, A. C., Kanter, L. R., Coppersmith, K. J. and Cornell, C. A. "The earthquakes of stable continental regions" vol. 1-5 (1994).

[40] Leppänen, T. "Re-evaluation of seismic hazard spectra in Loviisa NPP site" (2018), Fortum Power and Heat Oy. LO1-T84252-00007.

[41] Saari, J. and Malm, M. "Teollisuuden voima Oyj / Fortum Oyj, Re-evaluation of seismic hazard in Olkiluoto and Loviisa" (2016), ÅF-Consult Ltd. LO1-T84252-00004.

[42] Malm, M. and Kaisko, O. “Teollisuuden voima Oyj / Fortum Oyj, Re-evaluation of seismic hazard spectra in Olkiluoto and Loviisa” (2017), ÅF-Consult Ltd. LO1-T84252-00006.

[43] QGIS.org. QGIS Geographic Information System. QGIS Association (2023). http://www.qgis.org.

[44] Draper, N. R. and Smith, H. *Applied Regression Analysis*. John Wiley & Sons (1998).

[45] Slate Geotechnical Consultants, Inc. "Finland_PSHA_example_recurrence" (2021). [Unpublished Excel spreadsheet].

[46] Miller, A. C. and Rice, T. R. "Discrete approximation of probability distributions". *Management Science* 29.3 (1983), pp. 352–362.

[47] Electrical Power Research Institute (EPRI). "Use of cumulative absolute velocity (CAV) in determining effects of small magnitude earthquakes on seismic hazard analyses" (2006).

[48] Slate Geotechnical Consultants, Inc. "Comments on re-evaluation of seismic hazard at Loviisa and Olkiluoto NPP sites" (2001). LO1-T84252-00014Liite1

[49] Draw.io, version 23.1.2 (2024). [Online]. Available: https://app.diagrams.net (visited on 12/02/2024).

[50] Goulet, C. A., Bozorgnia, Y., Abrahamson, N. A., Kuehn, N., Al Atik, L., Youngs, R. R., Graves, R. W. and Atkinson, G. M. "Central and Eastern North America ground-motion characterization NGA-East final report" (2018). Pacific Earthquake Engineering Research Center at the University of California.

[51] Koskenranta, J., Leppänen, T. “Selvitys Loviisan voimalaitoksen suunnittelumaavastespektrin DBE2021 hyväksyttävyyteen liittyviin STUK vaatimuksiin” (2024), Fortum Power and Heat Oy. LO1-T84252-00022.

[52] Tiira, T., Uski, M., Kortström, J., Kaisko, O. and Korja, A. "Local seismic network for monitoring of a potential nuclear power plant area". *Journal of Seismology* 20 (2016), pp. 397-417.

[53] Ordaz, M., and Faccioli, E. "Modelling correlation between Gutenberg–Richter parameters a and b in PSHA". *Bulletin of Earthquake Engineering* 16 (2018), pp. 1829-1846.

# A Earthquake Recurrence/Completeness Analysis Without SSZ Groups

Table A1 summarizes the completeness analysis results conducted without any SSZ grouping. The number of earthquakes in each SSZ and magnitude bin after this completeness analysis are in Table A2. The corresponding recurrence parameters estimated with LS are in Table A3 and with MLE in Table A4. Figure A1 shows visual comparison between the estimated recurrence curves.

**Table A1:** First year of completeness interval by magnitude bin for the SSZs. All of the completeness intervals start from the first day of the given year and end at the end of 2021. This table summarizes the results for the completeness analysis which was conducted without any SSZ grouping

| | Magnitude Bin | | | | | |
|---|---|---|---|---|---|---|
| SSZ | 1.0-1.5 | 1.5-2.0 | 2.0-2.5 | 2.5-3.0 | 3.0-3.5 | 3.5- |
| 1 | 2007 | 1992 | 1962 | 1922 | 1742 | 1742 |
| 2 | 2002 | 1992 | 1992 | 1952 | 1882 | 1882 |
| 3 | - | 2002 | 1962 | 1882 | 1882 | 1882 |
| 4 | - | 2002 | 1962 | 1762 | 1742 | 1742 |
| 5 | 1997 | 1997 | 1962 | 1942 | 1882 | 1882 |
| 6 | 2012 | 2012 | 2012 | 1782 | 1782 | 1782 |
| 8 | 2012 | 2002 | 1882 | 1722 | 1722 | 1722 |
| 10 | 2007 | 2007 | 2002 | 1932 | 1932 | 1932 |

**Table A2:** Number of earthquakes by magnitude bin and SSZ, after filtering out earthquakes outside the completeness intervals defined in Table A1.

| | Magnitude Bin | | | | | | |
|---|---|---|---|---|---|---|---|
| SSZ | 1.0-1.5 | 1.5-2.0 | 2.0-2.5 | 2.5-3.0 | 3.0-3.5 | 3.5-4.0 | 4.0-4.5 |
| 1 | 29 | 25 | 20 | 13 | 9 | 2 | 1 |
| 2 | 122 | 64 | 23 | 11 | 8 | 3 | 0 |
| 3 | - | 41 | 44 | 21 | 6 | 2 | 0 |
| 4 | - | 20 | 14 | 25 | 10 | 3 | 0 |
| 5 | 365 | 141 | 61 | 33 | 19 | 4 | 1 |
| 6 (whole) | 30 | 14 | 4 | 13 | 6 | 1 | 1 |
| 6a | 14 | 1 | 2 | 4 | 0 | 0 | 0 |
| 6b | 10 | 5 | 0 | 4 | 1 | 1 | 0 |
| 6c | 6 | 8 | 2 | 5 | 5 | 0 | 1 |
| 8 | 33 | 23 | 36 | 19 | 11 | 5 | 1 |
| 10 | 62 | 17 | 8 | 5 | 0 | 0 | 0 |

**Table A3:** Recurrence parameters estimated with LS & Catalog completeness without SSZ groups (Table A1). $n_{\min}$ and its confidence bounds are defined for the minimum magnitude 4.5 Mw, used in the hazard calculations.

| SSZ | $b$ | $b_L$ | $b_U$ | $n_{\min}$ | $n_{\min,L}$ | $n_{\min,U}$ |
|---|---|---|---|---|---|---|
| 1 | 1.0109 | 0.7863 | 1.2355 | 0.0022133 | 0.0045336 | 0.0010805 |
| 2 | 1.0631 | 0.7862 | 1.3400 | 0.0035540 | 0.0105609 | 0.0011960 |
| 3 | 1.1716 | 0.7969 | 1.5463 | 0.0019281 | 0.0074592 | 0.0004984 |
| 4 | 1.0251 | 0.6967 | 1.3535 | 0.0020843 | 0.0068219 | 0.0006368 |
| 5 | 1.1457 | 0.8913 | 1.4001 | 0.0048104 | 0.0108356 | 0.0021355 |
| 6 | 1.0774 | 0.8377 | 1.3170 | 0.0016169 | 0.0034747 | 0.0007524 |
| 6a | 1.2407 | 0.7288 | 1.7526 | 0.0001666 | 0.0026384 | 0.0000105 |
| 6b | 1.0806 | 0.7434 | 1.4177 | 0.0004584 | 0.0016034 | 0.0001311 |
| 6c | 0.9188 | 0.6801 | 1.1576 | 0.0019490 | 0.0045457 | 0.0008357 |
| 8 | 1.0051 | 0.7815 | 1.2287 | 0.0025021 | 0.0051088 | 0.0012254 |
| 10 | 1.3162 | 0.7886 | 1.8438 | 0.0003548 | 0.0061174 | 0.0000206 |

**Table A4:** Recurrence parameters estimated with MLE & Catalog completeness without SSZ groups (Table A1). $n_{\min}$ and its confidence bounds are defined for the minimum magnitude 4.5 Mw, used in the hazard calculations.

| SSZ | $b$ | $b_L$ | $b_U$ | $n_{\min}$ | $n_{\min,L}$ | $n_{\min,U}$ |
|---|---|---|---|---|---|---|
| 1 | 0.9016 | 0.8084 | 0.9947 | 0.0024131 | 0.0046863 | 0.0012426 |
| 2 | 1.0161 | 0.9350 | 1.0972 | 0.0025718 | 0.0048259 | 0.0013706 |
| 3 | 1.1377 | 1.0011 | 1.2744 | 0.0012022 | 0.0028490 | 0.0005073 |
| 4 | 1.0080 | 0.8614 | 1.1547 | 0.0012906 | 0.0030681 | 0.0005429 |
| 5 | 1.0607 | 1.0082 | 1.1131 | 0.0041716 | 0.0062791 | 0.0027714 |
| 6 | 1.1070 | 0.9935 | 1.2205 | 0.0006129 | 0.0013788 | 0.0002725 |
| 6a | 1.3467 | 1.0930 | 1.6004 | 0.0000333 | 0.0002282 | 0.0000049 |
| 6b | 1.1614 | 0.9475 | 1.3753 | 0.0001276 | 0.0006033 | 0.0000270 |
| 6c | 0.9301 | 0.7640 | 1.0962 | 0.0007790 | 0.0023727 | 0.0002557 |
| 8 | 1.0414 | 0.9439 | 1.1388 | 0.0010243 | 0.0019680 | 0.0005332 |
| 10 | 1.2468 | 1.0869 | 1.4068 | 0.0002453 | 0.0008678 | 0.0000693 |

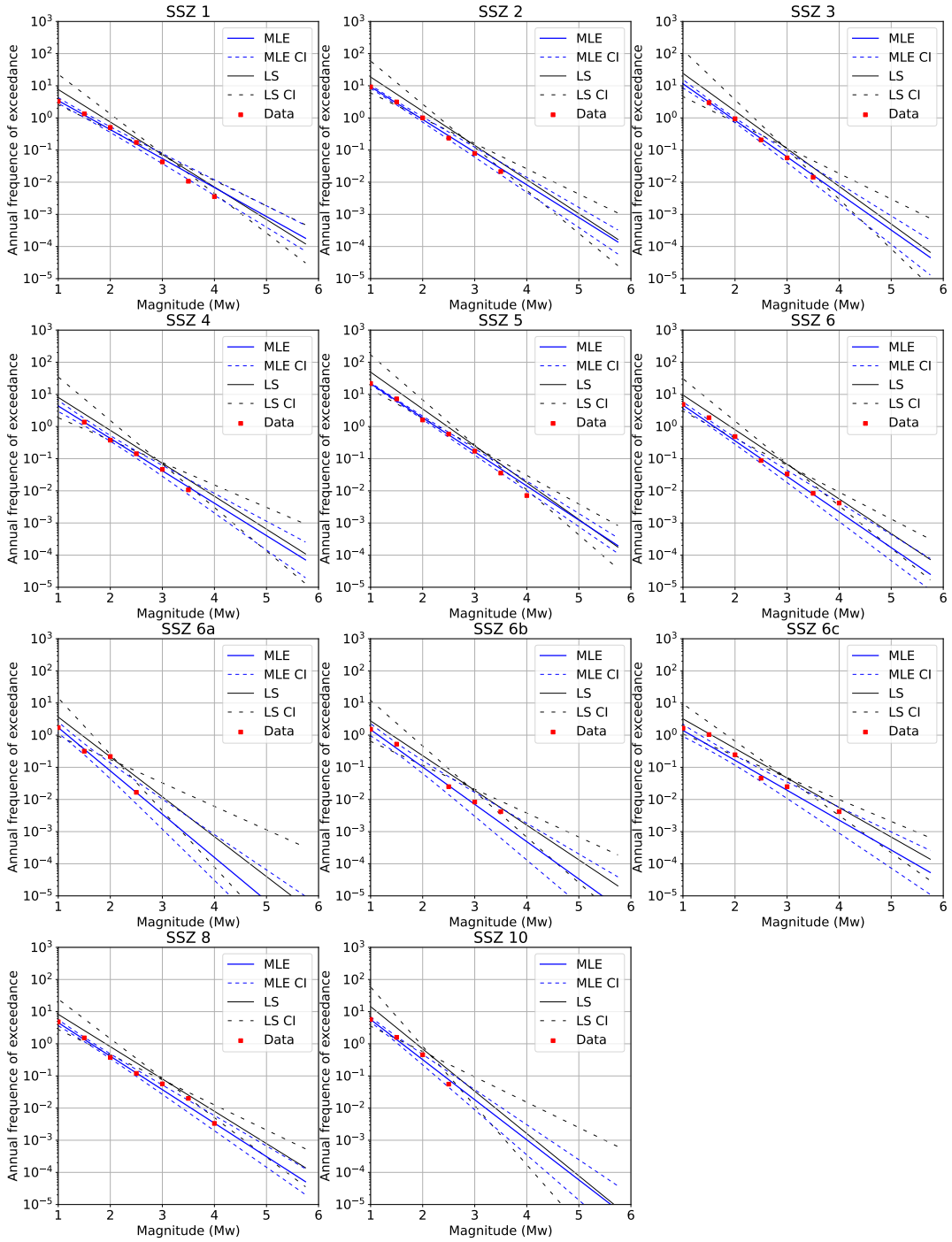


**Figure A1:** Recurrence curve means and confidence intervals (CI) calculated with LS and MLE, using the completeness intervals defined in Table A1. The cumulative datapoints are presented for the lower bound of the corresponding magnitude bin.

# B Loviisa Hazard Sensitivity

The Loviisa UHRS results for the different earthquake recurrence estimation methods and completeness analysis approaches are in this appendix. Table B1 shows the UHRS at different frequencies when the completeness analysis is conducted with SSZ groups and LS is used for the recurrence estimation. The results with the same completeness analysis, but when MLE is used instead of LS are in Table B2. Tables B3 and B4 show the corresponding results for LS and MLE, but with the completeness analysis conducted solely with the individual SSZs.

**Table B1:** Loviisa mean uniform hazard response spectra: Recurrence parameters estimated with LS & Catalog completeness with SSZ groups (Table 6).

| Frequency (Hz) | SA at mean AFE $10^{-3}$ (g) | SA at mean AFE $10^{-4}$ (g) | SA at mean AFE $10^{-5}$ (g) | SA at mean AFE $10^{-6}$ (g) | SA at mean AFE $10^{-7}$ (g) | SA at mean AFE $10^{-8}$ (g) |
|---|---|---|---|---|---|---|
| 0.10 | 0.00000 | 0.00005 | 0.00020 | 0.00063 | 0.00157 | 0.00348 |
| 0.13 | 0.00001 | 0.00009 | 0.00036 | 0.00112 | 0.00278 | 0.00611 |
| 0.20 | 0.00003 | 0.00021 | 0.00084 | 0.00244 | 0.00588 | 0.01260 |
| 0.25 | 0.00005 | 0.00035 | 0.00132 | 0.00375 | 0.00909 | 0.01942 |
| 0.33 | 0.00010 | 0.00063 | 0.00227 | 0.00646 | 0.01561 | 0.03435 |
| 0.40 | 0.00014 | 0.00093 | 0.00328 | 0.00927 | 0.02247 | 0.04922 |
| 0.50 | 0.00022 | 0.00148 | 0.00523 | 0.01428 | 0.03477 | 0.07484 |
| 0.67 | 0.00042 | 0.00253 | 0.00851 | 0.02343 | 0.05700 | 0.12076 |
| 1.00 | 0.00095 | 0.00515 | 0.01640 | 0.04530 | 0.10912 | 0.22823 |
| 1.33 | 0.00151 | 0.00799 | 0.02541 | 0.06936 | 0.16464 | 0.34169 |
| 2.00 | 0.00279 | 0.01311 | 0.04169 | 0.11487 | 0.27385 | 0.55163 |
| 2.50 | 0.00347 | 0.01613 | 0.05212 | 0.14400 | 0.34225 | 0.69081 |
| 3.33 | 0.00452 | 0.02055 | 0.06683 | 0.18806 | 0.44485 | 0.88023 |
| 4.00 | 0.00506 | 0.02296 | 0.07591 | 0.21927 | 0.51935 | 1.01972 |
| 5.00 | 0.00576 | 0.02673 | 0.09076 | 0.26590 | 0.61951 | 1.19431 |
| 10.00 | 0.00663 | 0.03406 | 0.13092 | 0.40524 | 0.95892 | 1.85096 |
| 13.33 | 0.00639 | 0.03483 | 0.14143 | 0.45384 | 1.07318 | 2.11088 |
| 25.00 | 0.00445 | 0.02725 | 0.12222 | 0.39538 | 0.94255 | 1.81980 |
| 33.33 | 0.00332 | 0.02059 | 0.09671 | 0.31140 | 0.74436 | 1.41344 |
| 50.00 | 0.00223 | 0.01386 | 0.06508 | 0.21264 | 0.50889 | 0.98638 |
| 100.00 | 0.00174 | 0.01075 | 0.04970 | 0.15654 | 0.37342 | 0.73656 |

**Table B2:** Loviisa mean uniform hazard response spectra: Recurrence parameters estimated with MLE & Catalog completeness with SSZ groups (Table 7).

| Frequency (Hz) | SA at mean AFE $10^{-3}$ (g) | SA at mean AFE $10^{-4}$ (g) | SA at mean AFE $10^{-5}$ (g) | SA at mean AFE $10^{-6}$ (g) | SA at mean AFE $10^{-7}$ (g) | SA at mean AFE $10^{-8}$ (g) |
|---|---|---|---|---|---|---|
| 0.10 | 0.00000 | 0.00001 | 0.00007 | 0.00025 | 0.00070 | 0.00154 |
| 0.13 | 0.00000 | 0.00002 | 0.00013 | 0.00045 | 0.00120 | 0.00267 |
| 0.20 | 0.00000 | 0.00006 | 0.00030 | 0.00101 | 0.00256 | 0.00542 |
| 0.25 | 0.00000 | 0.00011 | 0.00051 | 0.00154 | 0.00384 | 0.00817 |
| 0.33 | 0.00000 | 0.00018 | 0.00086 | 0.00261 | 0.00641 | 0.01348 |
| 0.40 | 0.00001 | 0.00027 | 0.00125 | 0.00372 | 0.00905 | 0.01888 |
| 0.50 | 0.00001 | 0.00047 | 0.00200 | 0.00585 | 0.01364 | 0.02902 |
| 0.67 | 0.00001 | 0.00081 | 0.00329 | 0.00928 | 0.02139 | 0.04565 |
| 1.00 | 0.00004 | 0.00171 | 0.00659 | 0.01718 | 0.03972 | 0.08545 |
| 1.33 | 0.00011 | 0.00279 | 0.01011 | 0.02615 | 0.05982 | 0.12966 |
| 2.00 | 0.00015 | 0.00490 | 0.01607 | 0.04164 | 0.09776 | 0.21706 |
| 2.50 | 0.00018 | 0.00607 | 0.01976 | 0.05136 | 0.12228 | 0.27734 |
| 3.33 | 0.00029 | 0.00776 | 0.02515 | 0.06483 | 0.15888 | 0.36184 |
| 4.00 | 0.00038 | 0.00853 | 0.02760 | 0.07281 | 0.18383 | 0.42463 |
| 5.00 | 0.00051 | 0.00977 | 0.03156 | 0.08574 | 0.22426 | 0.52047 |
| 10.00 | 0.00053 | 0.01120 | 0.03948 | 0.12123 | 0.34751 | 0.82557 |
| 13.33 | 0.00048 | 0.01098 | 0.04028 | 0.13061 | 0.39000 | 0.93903 |
| 25.00 | 0.00020 | 0.00784 | 0.03095 | 0.11177 | 0.34557 | 0.83184 |
| 33.33 | 0.00015 | 0.00586 | 0.02331 | 0.08696 | 0.27452 | 0.65457 |
| 50.00 | 0.00012 | 0.00387 | 0.01567 | 0.05868 | 0.18319 | 0.44316 |
| 100.00 | 0.00011 | 0.00308 | 0.01220 | 0.04435 | 0.13561 | 0.32532 |

**Table B3:** Loviisa mean uniform hazard response spectra: Recurrence parameters estimated with LS & Catalog completeness without SSZ groups (Table A3).

| Frequency (Hz) | SA at mean AFE $10^{-3}$ (g) | SA at mean AFE $10^{-4}$ (g) | SA at mean AFE $10^{-5}$ (g) | SA at mean AFE $10^{-6}$ (g) | SA at mean AFE $10^{-7}$ (g) | SA at mean AFE $10^{-8}$ (g) |
|---|---|---|---|---|---|---|
| 0.10 | 0.00001 | 0.00008 | 0.00033 | 0.00107 | 0.00268 | 0.00585 |
| 0.13 | 0.00002 | 0.00015 | 0.00062 | 0.00188 | 0.00475 | 0.01027 |
| 0.20 | 0.00005 | 0.00037 | 0.00142 | 0.00418 | 0.01013 | 0.02088 |
| 0.25 | 0.00010 | 0.00061 | 0.00229 | 0.00659 | 0.01538 | 0.03195 |
| 0.33 | 0.00016 | 0.00107 | 0.00399 | 0.01155 | 0.02777 | 0.05690 |
| 0.40 | 0.00024 | 0.00156 | 0.00586 | 0.01649 | 0.03934 | 0.07969 |
| 0.50 | 0.00042 | 0.00257 | 0.00934 | 0.02636 | 0.06091 | 0.12066 |
| 0.67 | 0.00074 | 0.00432 | 0.01533 | 0.04355 | 0.10087 | 0.19343 |
| 1.00 | 0.00160 | 0.00893 | 0.03090 | 0.08459 | 0.18540 | 0.35580 |
| 1.33 | 0.00267 | 0.01383 | 0.04867 | 0.12862 | 0.28488 | 0.53843 |
| 2.00 | 0.00478 | 0.02393 | 0.08139 | 0.21319 | 0.45678 | 0.84082 |
| 2.50 | 0.00603 | 0.03004 | 0.10390 | 0.27112 | 0.57249 | 1.04219 |
| 3.33 | 0.00786 | 0.03903 | 0.13310 | 0.34606 | 0.73218 | 1.29245 |
| 4.00 | 0.00877 | 0.04451 | 0.15318 | 0.40164 | 0.84451 | 1.49104 |
| 5.00 | 0.01024 | 0.05335 | 0.18574 | 0.48775 | 1.00538 | 1.77367 |
| 10.00 | 0.01256 | 0.07616 | 0.28654 | 0.74830 | 1.50628 | 2.72033 |
| 13.33 | 0.01257 | 0.08141 | 0.31475 | 0.83480 | 1.71192 | 3.10397 |
| 25.00 | 0.00961 | 0.06905 | 0.27778 | 0.72946 | 1.47278 | 2.66187 |
| 33.33 | 0.00728 | 0.05381 | 0.21751 | 0.57268 | 1.16416 | 2.09195 |
| 50.00 | 0.00486 | 0.03632 | 0.14600 | 0.38749 | 0.80726 | 1.40417 |
| 100.00 | 0.00373 | 0.02767 | 0.11162 | 0.29154 | 0.60221 | 1.06584 |

**Table B4:** Loviisa mean uniform hazard response spectra: Recurrence parameters estimated with MLE & Catalog completeness without SSZ groups (Table A4).

| Frequency (Hz) | SA at mean AFE $10^{-3}$ (g) | SA at mean AFE $10^{-4}$ (g) | SA at mean AFE $10^{-5}$ (g) | SA at mean AFE $10^{-6}$ (g) | SA at mean AFE $10^{-7}$ (g) | SA at mean AFE $10^{-8}$ (g) |
|---|---|---|---|---|---|---|
| 0.10 | 0.00000 | 0.00003 | 0.000131 | 0.00045 | 0.00124 | 0.00290 |
| 0.13 | 0.00000 | 0.00005 | 0.000233 | 0.00081 | 0.00219 | 0.00513 |
| 0.20 | 0.00001 | 0.00013 | 0.000576 | 0.00180 | 0.00475 | 0.01077 |
| 0.25 | 0.00002 | 0.00021 | 0.000926 | 0.00286 | 0.00741 | 0.01644 |
| 0.33 | 0.00003 | 0.00036 | 0.00157 | 0.00498 | 0.01281 | 0.02941 |
| 0.40 | 0.00004 | 0.00057 | 0.002338 | 0.00720 | 0.01838 | 0.04185 |
| 0.50 | 0.00010 | 0.00093 | 0.003731 | 0.01131 | 0.02900 | 0.06449 |
| 0.67 | 0.00016 | 0.00156 | 0.006264 | 0.01863 | 0.04828 | 0.10614 |
| 1.00 | 0.00039 | 0.00335 | 0.012565 | 0.03725 | 0.09419 | 0.19832 |
| 1.33 | 0.00069 | 0.00540 | 0.019689 | 0.05850 | 0.14306 | 0.30398 |
| 2.00 | 0.00127 | 0.00936 | 0.033737 | 0.10061 | 0.24414 | 0.49887 |
| 2.50 | 0.00160 | 0.01163 | 0.042838 | 0.12630 | 0.30659 | 0.62446 |
| 3.33 | 0.00215 | 0.01486 | 0.056111 | 0.16565 | 0.39914 | 0.80506 |
| 4.00 | 0.00247 | 0.01662 | 0.064068 | 0.19357 | 0.46907 | 0.93546 |
| 5.00 | 0.00279 | 0.01955 | 0.077351 | 0.23928 | 0.56580 | 1.10834 |
| 10.00 | 0.00312 | 0.02580 | 0.115031 | 0.36840 | 0.88530 | 1.71989 |
| 13.33 | 0.00298 | 0.02640 | 0.124546 | 0.41314 | 1.00354 | 1.98410 |
| 25.00 | 0.00202 | 0.02061 | 0.109587 | 0.36382 | 0.87983 | 1.70961 |
| 33.33 | 0.00150 | 0.01561 | 0.085578 | 0.28850 | 0.69339 | 1.33550 |
| 50.00 | 0.00105 | 0.01055 | 0.057993 | 0.19413 | 0.47256 | 0.92764 |
| 100.00 | 0.00083 | 0.00812 | 0.043612 | 0.14350 | 0.34662 | 0.68890 |

# C Olkiluoto Hazard Sensitivity

The Olkiluoto UHRS results for the different earthquake recurrence estimation methods and completeness analysis approaches are in this appendix. Table C1 shows the UHRS at different frequencies when the completeness analysis is conducted with SSZ groups and LS is used for the recurrence estimation. The results with the same completeness analysis, but when MLE is used instead of LS, are in Table C2. Tables C3 and C4 show the corresponding results for LS and MLE, but with the completeness analysis conducted solely with the individual SSZs.

**Table C1:** Olkiluoto mean uniform hazard response spectra: Recurrence parameters estimated with LS & Catalog completeness with SSZ groups (Table 6).

| Frequency (Hz) | SA at mean AFE $10^{-3}$ (g) | SA at mean AFE $10^{-4}$ (g) | SA at mean AFE $10^{-5}$ (g) | SA at mean AFE $10^{-6}$ (g) | SA at mean AFE $10^{-7}$ (g) | SA at mean AFE $10^{-8}$ (g) |
|---|---|---|---|---|---|---|
| 0.10 | 0.00001 | 0.00006 | 0.00023 | 0.00068 | 0.00153 | 0.00313 |
| 0.13 | 0.00002 | 0.00012 | 0.00042 | 0.00116 | 0.00266 | 0.00541 |
| 0.20 | 0.00005 | 0.00027 | 0.00094 | 0.00247 | 0.00547 | 0.01109 |
| 0.25 | 0.00009 | 0.00046 | 0.00145 | 0.00373 | 0.00831 | 0.01690 |
| 0.33 | 0.00015 | 0.00077 | 0.00245 | 0.00625 | 0.01396 | 0.02952 |
| 0.40 | 0.00022 | 0.00113 | 0.00348 | 0.00885 | 0.01972 | 0.04177 |
| 0.50 | 0.00037 | 0.00178 | 0.00547 | 0.01344 | 0.03039 | 0.06394 |
| 0.67 | 0.00066 | 0.00294 | 0.00865 | 0.02116 | 0.04869 | 0.10397 |
| 1.00 | 0.00138 | 0.00581 | 0.01599 | 0.03940 | 0.09152 | 0.19165 |
| 1.33 | 0.00225 | 0.00884 | 0.02407 | 0.05903 | 0.13702 | 0.29197 |
| 2.00 | 0.00385 | 0.01395 | 0.03789 | 0.09504 | 0.22543 | 0.46985 |
| 2.50 | 0.00485 | 0.01687 | 0.04616 | 0.11765 | 0.28299 | 0.58767 |
| 3.33 | 0.00607 | 0.02100 | 0.05771 | 0.15051 | 0.36246 | 0.75376 |
| 4.00 | 0.00664 | 0.02310 | 0.06425 | 0.17247 | 0.42119 | 0.86906 |
| 5.00 | 0.00753 | 0.02632 | 0.07476 | 0.20740 | 0.51019 | 1.03252 |
| 10.00 | 0.00828 | 0.03145 | 0.10202 | 0.31155 | 0.78263 | 1.56013 |
| 13.33 | 0.00791 | 0.03158 | 0.10801 | 0.34339 | 0.87636 | 1.77943 |
| 25.00 | 0.00541 | 0.02368 | 0.09003 | 0.30065 | 0.76734 | 1.53081 |
| 33.33 | 0.00401 | 0.01778 | 0.06908 | 0.23867 | 0.60169 | 1.20624 |
| 50.00 | 0.00272 | 0.01201 | 0.04702 | 0.15888 | 0.40805 | 0.83691 |
| 100.00 | 0.00219 | 0.00946 | 0.03582 | 0.12029 | 0.30508 | 0.62379 |

**Table C2:** Olkiluoto mean uniform hazard response spectra: Recurrence parameters estimated with MLE & Catalog completeness with SSZ groups (Table 7).

| Frequency (Hz) | SA at mean AFE $10^{-3}$ (g) | SA at mean AFE $10^{-4}$ (g) | SA at mean AFE $10^{-5}$ (g) | SA at mean AFE $10^{-6}$ (g) | SA at mean AFE $10^{-7}$ (g) | SA at mean AFE $10^{-8}$ (g) |
|---|---|---|---|---|---|---|
| 0.10 | 0.00000 | 0.00003 | 0.00013 | 0.00040 | 0.00099 | 0.00190 |
| 0.13 | 0.00000 | 0.00006 | 0.00022 | 0.00070 | 0.00162 | 0.00323 |
| 0.20 | 0.00002 | 0.00014 | 0.00054 | 0.00145 | 0.00331 | 0.00644 |
| 0.25 | 0.00003 | 0.00022 | 0.00084 | 0.00226 | 0.00504 | 0.00964 |
| 0.33 | 0.00005 | 0.00039 | 0.00138 | 0.00366 | 0.00815 | 0.01561 |
| 0.40 | 0.00010 | 0.00059 | 0.00200 | 0.00523 | 0.01125 | 0.02177 |
| 0.50 | 0.00015 | 0.00097 | 0.00315 | 0.00800 | 0.01673 | 0.03289 |
| 0.67 | 0.00026 | 0.00157 | 0.00505 | 0.01207 | 0.02573 | 0.05045 |
| 1.00 | 0.00064 | 0.00321 | 0.00951 | 0.02178 | 0.04533 | 0.09089 |
| 1.33 | 0.00106 | 0.00503 | 0.01377 | 0.03165 | 0.06597 | 0.13482 |
| 2.00 | 0.00184 | 0.00822 | 0.02162 | 0.04844 | 0.10187 | 0.21731 |
| 2.50 | 0.00239 | 0.00999 | 0.02609 | 0.05796 | 0.12508 | 0.27261 |
| 3.33 | 0.00300 | 0.01203 | 0.03146 | 0.07096 | 0.15836 | 0.35053 |
| 4.00 | 0.00326 | 0.01297 | 0.03412 | 0.07816 | 0.17987 | 0.40742 |
| 5.00 | 0.00367 | 0.01445 | 0.03835 | 0.08966 | 0.21370 | 0.49571 |
| 10.00 | 0.00393 | 0.01608 | 0.04599 | 0.11986 | 0.31809 | 0.77222 |
| 13.33 | 0.00368 | 0.01562 | 0.04646 | 0.12691 | 0.35189 | 0.86967 |
| 25.00 | 0.00252 | 0.01106 | 0.03491 | 0.10370 | 0.30796 | 0.76760 |
| 33.33 | 0.00180 | 0.00832 | 0.02632 | 0.07961 | 0.24464 | 0.60211 |
| 50.00 | 0.00123 | 0.00559 | 0.01763 | 0.05375 | 0.16269 | 0.40705 |
| 100.00 | 0.00104 | 0.00451 | 0.01390 | 0.04126 | 0.12220 | 0.30271 |

**Table C3:** Olkiluoto mean uniform hazard response spectra: Recurrence parameters estimated with LS & Catalog completeness without SSZ groups (Table A3).

| Frequency (Hz) | SA at mean AFE $10^{-3}$ (g) | SA at mean AFE $10^{-4}$ (g) | SA at mean AFE $10^{-5}$ (g) | SA at mean AFE $10^{-6}$ (g) | SA at mean AFE $10^{-7}$ (g) | SA at mean AFE $10^{-8}$ (g) |
|---|---|---|---|---|---|---|
| 0.10 | 0.00002 | 0.00008 | 0.00029 | 0.00082 | 0.00183 | 0.00383 |
| 0.13 | 0.00003 | 0.00015 | 0.00053 | 0.00140 | 0.00319 | 0.00669 |
| 0.20 | 0.00007 | 0.00035 | 0.00115 | 0.00297 | 0.00665 | 0.01368 |
| 0.25 | 0.00012 | 0.00058 | 0.00177 | 0.00456 | 0.01020 | 0.02114 |
| 0.33 | 0.00020 | 0.00098 | 0.00299 | 0.00770 | 0.01744 | 0.03715 |
| 0.40 | 0.00030 | 0.00140 | 0.00428 | 0.01087 | 0.02500 | 0.05286 |
| 0.50 | 0.00053 | 0.00226 | 0.00669 | 0.01662 | 0.03835 | 0.08066 |
| 0.67 | 0.00090 | 0.00364 | 0.01058 | 0.02670 | 0.06205 | 0.12885 |
| 1.00 | 0.00184 | 0.00717 | 0.01979 | 0.05049 | 0.11711 | 0.24488 |
| 1.33 | 0.00295 | 0.01080 | 0.02978 | 0.07633 | 0.17707 | 0.36243 |
| 2.00 | 0.00507 | 0.01706 | 0.04761 | 0.12361 | 0.28983 | 0.58037 |
| 2.50 | 0.00619 | 0.02079 | 0.05854 | 0.15466 | 0.36217 | 0.72717 |
| 3.33 | 0.00777 | 0.02598 | 0.07421 | 0.20112 | 0.47028 | 0.92114 |
| 4.00 | 0.00845 | 0.02843 | 0.08368 | 0.23384 | 0.54441 | 1.05957 |
| 5.00 | 0.00952 | 0.03238 | 0.09898 | 0.27980 | 0.64890 | 1.24039 |
| 10.00 | 0.01050 | 0.04011 | 0.14079 | 0.42552 | 0.99846 | 1.92115 |
| 13.33 | 0.01011 | 0.04082 | 0.15179 | 0.47588 | 1.11012 | 2.17650 |
| 25.00 | 0.00696 | 0.03160 | 0.12990 | 0.41219 | 0.97546 | 1.87777 |
| 33.33 | 0.00523 | 0.02396 | 0.10257 | 0.32348 | 0.76881 | 1.45407 |
| 50.00 | 0.00350 | 0.01617 | 0.06929 | 0.22254 | 0.52563 | 1.01449 |
| 100.00 | 0.00285 | 0.01260 | 0.05283 | 0.16363 | 0.38771 | 0.76051 |

**Table C4:** Olkiluoto mean uniform hazard response spectra: Recurrence parameters estimated with MLE & Catalog completeness without SSZ groups (Table A4).

| Frequency (Hz) | SA at mean AFE $10^{-3}$ (g) | SA at mean AFE $10^{-4}$ (g) | SA at mean AFE $10^{-5}$ (g) | SA at mean AFE $10^{-6}$ (g) | SA at mean AFE $10^{-7}$ (g) | SA at mean AFE $10^{-8}$ (g) |
|---|---|---|---|---|---|---|
| 0.10 | 0.00000 | 0.00004 | 0.00017 | 0.00052 | 0.00119 | 0.00235 |
| 0.13 | 0.00001 | 0.00008 | 0.00030 | 0.00089 | 0.00200 | 0.00398 |
| 0.20 | 0.00003 | 0.00019 | 0.00070 | 0.00183 | 0.00408 | 0.00807 |
| 0.25 | 0.00005 | 0.00031 | 0.00109 | 0.00282 | 0.00618 | 0.01220 |
| 0.33 | 0.00010 | 0.00056 | 0.00178 | 0.00464 | 0.01021 | 0.02066 |
| 0.40 | 0.00015 | 0.00081 | 0.00260 | 0.00654 | 0.01415 | 0.02910 |
| 0.50 | 0.00024 | 0.00130 | 0.00403 | 0.01003 | 0.02156 | 0.04456 |
| 0.67 | 0.00045 | 0.00214 | 0.00639 | 0.01519 | 0.03358 | 0.07098 |
| 1.00 | 0.00099 | 0.00425 | 0.01184 | 0.02791 | 0.06182 | 0.13208 |
| 1.33 | 0.00154 | 0.00653 | 0.01736 | 0.04099 | 0.09314 | 0.20227 |
| 2.00 | 0.00278 | 0.01052 | 0.02741 | 0.06442 | 0.14986 | 0.32867 |
| 2.50 | 0.00341 | 0.01250 | 0.03278 | 0.07894 | 0.18932 | 0.41629 |
| 3.33 | 0.00433 | 0.01520 | 0.04013 | 0.09947 | 0.24830 | 0.54155 |
| 4.00 | 0.00476 | 0.01647 | 0.04394 | 0.11219 | 0.28494 | 0.62741 |
| 5.00 | 0.00536 | 0.01846 | 0.05004 | 0.13282 | 0.34187 | 0.75642 |
| 10.00 | 0.00571 | 0.02093 | 0.06345 | 0.19552 | 0.53604 | 1.15780 |
| 13.33 | 0.00538 | 0.02046 | 0.06560 | 0.21428 | 0.59905 | 1.30446 |
| 25.00 | 0.00354 | 0.01457 | 0.05196 | 0.18459 | 0.52906 | 1.14731 |
| 33.33 | 0.00269 | 0.01097 | 0.03960 | 0.14332 | 0.41244 | 0.91337 |
| 50.00 | 0.00176 | 0.00740 | 0.02667 | 0.09990 | 0.28241 | 0.62158 |
| 100.00 | 0.00145 | 0.00596 | 0.02070 | 0.07408 | 0.20902 | 0.46298 |